



Słowakiewicz, M., Blumenberg, M., Więclaw, D., Röhling, H. G., Scheeder, G., Hindenberg, K., Leśniak, A., Idiz, E., Tucker, M., Pancost, R., Kotarba, M. J., & Gerling, J. P. (2018). Zechstein Main Dolomite oil characteristics in the Southern Permian Basin: I. Polish and German sectors. *Marine and Petroleum Geology*, 93, 356-375. <https://doi.org/10.1016/j.marpetgeo.2018.03.023>

Peer reviewed version

License (if available):  
CC BY-NC-ND

Link to published version (if available):  
[10.1016/j.marpetgeo.2018.03.023](https://doi.org/10.1016/j.marpetgeo.2018.03.023)

[Link to publication record in Explore Bristol Research](#)  
PDF-document

This is the author accepted manuscript (AAM). The final published version (version of record) is available online via <https://www.sciencedirect.com/science/article/pii/S0264817218301235> . Please refer to any applicable terms of use of the publisher.

## University of Bristol - Explore Bristol Research

### General rights

This document is made available in accordance with publisher policies. Please cite only the published version using the reference above. Full terms of use are available: <http://www.bristol.ac.uk/red/research-policy/pure/user-guides/ebr-terms/>

Zechstein Main Dolomite oil characteristics in the Southern Permian Basin: I. Polish and German sectors

Mirosław Słowakiewicz<sup>1,2,3</sup>, Martin Blumenberg<sup>4</sup>, Dariusz Więclaw<sup>5</sup>, Heinz-Gerd Röhling<sup>6</sup>, Georg Scheeder<sup>4</sup>, Katja Hindenberg<sup>7</sup>, Andrzej Leśniak<sup>5</sup>, Erdem F. Idiz<sup>8</sup>, Maurice E. Tucker<sup>9</sup>, Richard D. Pancost<sup>1,3</sup>, Maciej J. Kotarba<sup>5</sup>, Johannes P. Gerling<sup>4</sup>

<sup>1</sup>Faculty of Geology, University of Warsaw, ul. Żwirki i Wigury 93, 02-089 Warszawa, Poland

<sup>2</sup>Organic Geochemistry Unit, School of Chemistry, University of Bristol, Cantock's Close, Bristol, BS8 1TS, UK; e-mail: m.slowakiewicz@gmail.com

<sup>3</sup>Cabot Institute, University of Bristol, Cantock's Close, Bristol, BS8 1UJ, UK

<sup>4</sup>Federal Institute for Geosciences and Natural Resources (BGR), Stilleweg 2, 30655 Hannover, Germany

<sup>5</sup>AGH University of Science and Technology, Faculty of Geology, Geophysics and Environmental Protection, Al. Mickiewicza 30, 30-059 Kraków, Poland

<sup>6</sup>State Authority for Mining, Energy and Geology, Geological Survey of Lower Saxony, Stilleweg 2, 30655 Hannover, Germany

<sup>7</sup>Institute of Bio- and Geosciences (IBG-3), Forschungszentrum Jülich GmbH, 52425 Jülich, Germany

<sup>8</sup>Department of Earth Sciences, University of Oxford, South Parks Road, Oxford, OX1 3AN, UK

<sup>9</sup>School of Earth Sciences, University of Bristol, BS8 1RJ, UK

## Highlights

Main Dolomite oils from Germany and Poland constitute ten distinct groups

Aromatic C<sub>40</sub> carotenoids are important correlative biomarker tools

Main Dolomite oils were generated from algal-rich marly carbonate/evaporite source rocks

## Abstract

Geochemical analyses were used to classify 39 Zechstein (Late Permian, Lopingian) Main Dolomite (Ca<sub>2</sub>) crude oil samples from fields in the eastern and southern sector of the

Southern Permian Basin (SPB) of Europe and to provide new insights into the origin of the oil. Geochemical data indicate that Ca2 oils were generated in the early-to-late oil window and are mostly non-waxy oils. Various biomarker and stable carbon isotopic ratios were used to identify source and depositional settings for source rocks of Ca2 oils arranged within 10 distinct oil groups. Specifically, the geochemical analyses and oil-oil correlations revealed a set of characteristic biomarkers including an even-over-odd predominance (EOP) for the C<sub>20-30</sub> *n*-alkanes, C<sub>40</sub> carotenoid occurrence (isorenieratane, chlorobactane,  $\beta$ -isorenieratane), bisnorhopane/hopane (BNH/H) ratios >0.1, high abundances of C<sub>35</sub> homohopanes and elevated concentrations of C<sub>32</sub> and C<sub>34</sub> homohopanes, a predominance of C<sub>29</sub> homologues among 4-desmethyl steranes in the majority of oil samples, and a high abundance of diasteranes. Stable carbon isotopes and biomarkers provided ample evidence that Ca2 oils were generated from predominantly algal-rich marly carbonate/evaporite source rocks located in the lower slope/shallow-basin and lagoonal facies of the Ca2 basin, all deposited under suboxic-anoxic (euxinic) conditions. In the case of all higher maturity oils, the source rocks could not be reliably identified but high (>2) C<sub>24</sub>Tet/C<sub>23</sub> values suggest a carbonate-evaporite depositional setting.

## 1. Introduction

The intracontinental Southern Permian Basin (SPB, Fig. 1) is the southern sub-basin of the Central European Basin (CEB) and one of the richest and most extensively studied petroliferous basins in Europe. It is Europe's largest sedimentary basin, evolving from the latest Carboniferous to Recent times (van Wees et al., 2000; Pharaoh et al., 2010), and extending over ~1,700 km from eastern England to the Belarussian-Polish and Polish-Lithuanian borders, and from Denmark to southern Germany, covering an area of ~ 700,000 km<sup>2</sup>, in Zechstein Limestone [Ca1] time. The SPB oil is predominantly reservoirized in porous and fractured carbonate facies of the Zechstein Main Dolomite (Ca2; also called the Staßfurt Karbonat in Germany) and it is believed to have been derived from Ca2 basin, slope and lagoon facies.

During Late Permian (Zechstein) greenhouse time, the SPB was repeatedly subjected to marine transgressions and regressions which resulted in the succession having a cyclic character of carbonate and evaporite deposits. Of these the second carbonate cycle (Ca2; Fig. 2) is economically the most important. Since the discovery of the Volkenroda field in 1930 in

Germany (Albrecht, 1932), about 258 additional fields have been discovered, including two large Ca<sub>2</sub> fields in Poland: Barnówko-Mostno-Buszewo (1992; ~94 Mbo), and Lubiatów-Międzychód-Grotów (2001-2003; ~48 Mbo) (Doornenbal and Stevenson, 2010). The underlying and overlying evaporite rocks enclose the Ca<sub>2</sub> (Kovalevych et al., 2008) and create an effective seal for hydrocarbons trapped in the Ca<sub>2</sub> reservoir.

Although the Ca<sub>2</sub> gas accumulations and their origin are relatively well understood (Krooss et al., 1995, 2005, 2006; Mingram et al., 2005; Jurisch and Krooss, 2008; Zdanowski and Wozniak, 2010; Kotarba et al., 2017), there are still many uncertainties concerning Ca<sub>2</sub> oil-oil correlations and correlations of Ca<sub>2</sub> oils to potential source rocks (Hofmann and Leythaeuser, 1995; Gerling et al., 1996a; Czechowski and Piela, 1997; Wehner, 1997; Czechowski et al., 1998; Kotarba et al., 1998, 2000; Hindenberg, 1999; Grelowski and Czechowski, 2010; Mikołajewski et al., 2012; Hammes et al., 2014; Petersen et al., 2016). Furthermore, the lack of sufficient information prevents the establishment of oil families, an understanding of their origin, the prediction of migration routes and possible secondary processes.

In this paper, we integrate the available and newly-generated molecular and isotopic compositions of the Ca<sub>2</sub> oils and identify their characteristic biomarkers. We evaluate the occurrence of the aromatic C<sub>40</sub> carotenoids (i.e., chlorobactane, isorenieratane) which can be used to infer water column stratification and photic zone euxinia (PZE, Summons and Powell, 1986; Sinninghe Damsté et al., 1993). Our conclusions are integrated with other biomarker signatures to interpret past redox conditions and organic matter (OM) source, using stable carbon isotopes of saturated and aromatic fractions as well as distributions of *n*-alkanes, isoprenoids, tricyclic terpanes, hopanes and steranes. These data and interpretations are complemented by the conclusions on the origin of Ca<sub>2</sub> oils derived from the pioneering work of Gerling et al. (1996a), subsequently continued by others (e.g., Czechowski et al., 1998; Kotarba et al., 1998, 2000, 2003; Hindenberg, 1999; Kotarba and Wagner, 2007; Grelowski and Czechowski, 2010; Słowakiewicz and Gąsiewicz, 2013).

## **2. Geological setting**

In the Permian, the CEB mainly consisted of two WNW – ESE striking basins, called the Northern and Southern Permian basins (NPB and SPB). During sedimentation of the

Zechstein Group, which represents approximately ~2 to 2.6 m.y. (Changhsingian; Szurlies, 2013; Hounslow and Balabanov *in press*), the SPB was located in northern Pangea at palaeolatitudes of 10-15°N. It was separated from the NPB by a chain of palaeo-highs, i.e., the Mid North Sea High and Ringkøbing-Fyn High (Fig. 1), both of which were covered by sediments during the latest Zechstein (Hiete et al., 2005). The NPB and the SPB were both occupied by waters of the epicontinental Zechstein Sea. Marine ingressions from the Boreal Sea and the Palaeo-Tethys into the mainly restricted basins resulted in deposition of a thick, cyclic succession (as much as ~2 km) of bedded carbonate, sulphate and halite with minor potash salt and with relatively thin intercalations of clastic sediments (Richter-Bernburg, 1953; Taylor, 1998; Paul, 2010). Four major carbonate-evaporite cycles (Z1-Z4) are recognised across the SPB, overlain by three thinner clastic-evaporite cycles (Z5-Z7), reflecting a more regressive trend in the upper part with an increase of fluvial deposits delivered from surrounding highlands to the basin centre. Only in the central parts of the North German sub-Basin (NGB) do the upper three cycles contain halite (Best, 1989). Many sulphate evaporites of the Zechstein Group resemble those of the modern Abu Dhabi and Qatar sabkhas, whereas the configuration of the basin and its seawater circulation may have resembled that of the present-day Mediterranean Sea.

### **3. Potential source rock settings within the Ca<sub>2</sub> strata**

Previously invoked concepts for potential source rocks of Ca<sub>2</sub> oils have evolved over the past 20 years, from models invoking lower slope-basinal facies (Karnin et al., 1996; Kotarba et al., 2003) to inner platform-slope-lagoonal facies (Pletsch et al., 2010) to lagoonal and lower slope-shallow basin facies containing mixed algal-microbial-terrigenous types of OM with relatively low total organic carbon (TOC) content (Gerling et al., 1996a; Schwark et al., 1998; Hindenberg, 1999; Kotarba and Wagner, 2007; Słowakiewicz and Mikołajewski, 2011; Słowakiewicz and Gąsiewicz, 2013; Słowakiewicz et al., 2013, 2015, 2016a; Kosakowski and Krajewski, 2014, 2015). Recently, biomarker studies have helped to characterise the palaeoenvironmental and palaeoceanographic conditions during the deposition of Ca<sub>2</sub> facies (Słowakiewicz et al., 2015, 2016a), and suggested characteristic biomarkers and biomarker ratios for the individual facies types (Słowakiewicz, 2016).

As previously postulated (e.g., Gerling et al., 1996b; Karnin et al., 1996; Czechowski et al., 1998; Kotarba et al., 1998, 2000, 2003; Hindenberg, 1999; Kotarba and Wagner, 2007;

Słowakiewicz and Gąsiewicz, 2013), the Ca2 intraformationally generated oil, which migrated to fill pores, fissures, fractures and karst cavities (Słowakiewicz et al., 2016b); this resulted in an artificially-enhanced enrichment in OM volumes for the Ca2 sequence as a whole. This process is evident in the elevated Rock-Eval production index (PI) values (PI>0.4), which were interpreted by Kotarba et al. (2003) as implying that >30% of their overall Ca2 rock sample population was impregnated by migrated hydrocarbons.

## **4. Materials and Methods**

### *4.1. Sample collection*

Thirty-nine crude oil samples were collected from 1) NW Poland (Kamień Pomorski and Pomerania carbonate platforms) and SW Poland (west Fore-Sudetic Monocline), which were situated on the northern and southern margins of the SPB, respectively (Fig. 2a,b); 2) NE Germany (Mecklenburg-Vorpommern) and SE Germany (Brandenburg), which were parts of the NGB situated on the northern and southern margins of the SPB (Fig. 2a,b); and 3) the northern part of the Thuringian (sub)-Basin (TB, Germany), which was located on the south-central margin of the SPB (Fig. 2c). Two crude oils (PL-4 and -5) are reservoired in Zechstein Platy Dolomite (Ca3) facies but due to the geochemical similarity to the Ca2 oils they are included in our overall dataset.

### *4.2. Extraction and biomarker analyses*

About 5 - 100 mg of the stabilized crude oil samples were subjected to a fractionation procedure. Prior to this, asphaltenes were precipitated over 12 h by adding 2 mL dichloromethane (DCM) and 60 mL petroleum ether to (at maximum) 100 mg of sample. Subsequently, the mixtures were centrifuged at 3000 rpm for 15 min. The supernatant solution containing maltenes was collected and the solvent removed through evaporation in a nitrogen atmosphere at 35 °C. Parallel asphaltene precipitation of a sample of known composition (Norwegian Geochemical Standard NSO-1 oil) for every sample sequence assured reproducibility control of the method. The residual maltenes (up to 100 mg) were separated into aliphatic and aromatic fractions as well as into hetero-compounds (NSO-compounds) on silica gel (activated at 240 °C for 12 h) by mid-pressure liquid chromatography (BESTA-Technik für Chromatographie GmbH), using a sequence of organic solvents of different polarity (iso-hexane, iso-hexane/DCM (2:1; v:v), DCM/MeOH (2:1; v:v).

The distribution of compounds contained in the aliphatic and aromatic fractions was determined with gas chromatography-mass spectrometry (GC-MS), using an Agilent-7890

instrument equipped with a PTV inlet splitting on two DB-1 columns (each 50 m; 0.2 mm i.d.; film thickness 0.11  $\mu\text{m}$ ), one coupled to a flame ionisation detector (FID), the other one to an Agilent 7000 QQQ mass spectrometer (in Germany); and an Agilent 7890A equipped with a fused silica capillary column (60 m, 0.25 mm i.d.) coated with 95 % methyl-/5 % phenylsiloxane phase (DB-5MS, film thickness 0.25  $\mu\text{m}$ ) and coupled with an Agilent 5975C mass selective detector (in Poland). Helium was used as the carrier gas. The columns were heated from 60 °C to 150 °C, at a rate of 20 °C min<sup>-1</sup>, then heated to 320 °C, at a rate of 4.5 °C min<sup>-1</sup> (held for 15 min). Measurements of aliphatic fractions were carried out using parent-daughter-scans via multiple-reaction-monitoring (MRM). Aromatic fractions were analysed in full-scan mode. Peak ratio calculations for GC-FID and GC-MS were done from integrated area:area and the biomarker ratios were computed as area:area as well. Isorenieratane was identified from co-elution experiments with an aliphatic fraction from the Rhaetian Kössen Formation, Germany and the Changhsingian Main Dolomite, Poland (and the presence of spectral characteristics typical for aryl isoprenoids; e.g.  $m/z$  133; Grice et al., 1996; Koopmans et al., 1996; Słowakiewicz et al., 2015). Quantification was achieved through comparison of the FID trace of the isorenieratane peak of the sample with an  $n\text{-C}_{40}$  alkane calibration sample set with known concentrations.

#### 4.3. Stable carbon isotope analyses

Stable carbon isotope ratios of the  $\text{C}_{15+}$  saturated and aromatic hydrocarbon fractions were determined after combustion (Schoell, 1984) using a Dual-Inlet VG-903 isotope mass spectrometer. The  $\delta^{13}\text{C}$  values are reported relative to the Vienna Pee Dee Belemnite (VPDB) standard, and the analytical error, determined by using co-injected standards, is  $\pm 0.2\text{‰}$ .

### 5. Results and discussion

Several parameters were excluded from analysis because they are readily altered by thermal maturity: API gravity, sulphur content, saturated/aromatic hydrocarbon ratio, and the weight percent  $<\text{C}_{15}$  hydrocarbon fraction.

#### 5.1. Maturity

The thermal maturity of oils (Table 1, 2) was evaluated based on analysis of the saturated and aromatic hydrocarbons including ratios of pristane/ $n$ -heptadecane ( $\text{Pr}/n\text{-C}_{17}$ ) and

phytane/*n*-octadecane (Ph/*n*-C<sub>18</sub>), C<sub>27</sub> 18 $\alpha$ -trisorneohopane (Ts) to C<sub>27</sub> 17 $\alpha$ -trisnorhopane (Tm) (Ts/( Tm), C<sub>27</sub> diasteranes /(diasteranes + regular steranes) vs Ts/Tm (controlled by thermal maturity and source, Moldowan et al., 1994), C<sub>30</sub> moretane/C<sub>30</sub> hopane (M/H), 20S/(20S+20R) for  $\alpha\alpha\alpha$ C<sub>29</sub> steranes,  $\beta\beta/(\alpha\alpha + \beta\beta)$  for  $\alpha\beta\beta$ C<sub>29</sub> steranes, triaromatic steroids (TA[I]/TA[I+II]), 4- to 1-methyldibenzothiophene (MDR), and the calculated vitrinite reflectance ( $R_m = 0.073 \times MDR + 0.51$ , Radke, 1988). Using a variety of maturity parameters can help to overcome possible fractionation effects resulting from adsorption of OM on mineral surfaces, the expulsion process, and subsequent migration of oil (Zhusheng et al., 1988), all of which may affect maturation signatures and variations in biomarker distributions.

The isoprenoid-based ratios Pr/*n*-C<sub>17</sub> and Ph/*n*-C<sub>18</sub> show values of 0.07 – 1.17 and 0.2 – 1.5, respectively (Table 1, Fig. 3). As a result of the preferential release of *n*-alkanes during maturation, these ratios decrease with increasing thermal stress, but they also can be affected by organofacies variation and biodegradation (Peters et al., 2005). These ratios are the lowest, respectively, in BGR-13 and PL-6 and the highest in PL-5 (Table 1). The Pr/*n*-C<sub>17</sub> ratio shows groupings of Ca2 oils (Fig. 3) most likely resulting from different thermal maturity of OM.

The Ts/Tm ratios range from 0.6 – 11.8 and are the highest (>4) in BGR-9, PL-12, -18 and -19, and this ratio appears to have been maturity-controlled in the Ca2 oil samples (Fig. 4a). However, it can also be affected by lithology: in carbonate settings Tm is preferentially generated (Peters et al., 2005). The moretane/hopane (M/H) ratios vary between 0.05 and 0.19 in all samples (Table 2). The M/H ratios could not be determined in BGR-9, PL-18, -19, and -24 due to the presence of only trace amounts of these biomarkers.

The isomerisation equilibrium for  $\beta\beta/(\alpha\alpha + \beta\beta)$  and 20S/(20S+20R) C<sub>29</sub> steranes lies between 0.67 – 0.71 and 0.52 – 0.57, respectively (Seifert and Moldowan, 1986). Both parameters are valid through peak oil generation. In our samples, values for the  $\beta\beta/(\alpha\alpha + \beta\beta)$  ratio vary between 0.52 and 0.62, whereas the 20S/(20S+20R) values range from 0.43 to 0.56, indicating generation from the early oil phase to peak oil window (Table 2). Huang et al. (1990) noted that oils derived from gypsum, rock salt and carbonate -enriched source rocks show lower  $\beta\beta/(\alpha\alpha + \beta\beta)$  values than for 20S/(20S+20R). Hence, the  $\beta\beta/(\alpha\alpha + \beta\beta)$  C<sub>29</sub> sterane ratio may not be reliable as a direct maturity indicator because it could be affected by source rock lithology. The TA(I)/TA(I+II) ratio (Mackenzie et al., 1981) increases with increasing



maturity (Beach et al., 1989) and is descriptive for mature and late mature stages of oil generation (Peters et al., 2005). Values for TA(I)/TA(I+II) ratio are between 0.04 and 1 indicating generation from the peak oil phase to late oil window (Table 2).

MDR values in the studied samples vary between 1.5 and 8.3 giving maturities in the range of 0.6%Rm to 1.1%Rm (Fig. 4b, Table 2), indicating early to peak/late oil window generation.

Collectively, our data indicate that the majority of oil samples were generated in the peak oil window, whereas seven oils located in SE NGB (BGR-6, -7, -8, -9), NW (PL-18, -19) and SW (PL-24) Poland were generated in the late oil window (Fig. 2, Table 2), which suggests a different thermal history. In addition, the maturity estimation for BGR-1 is inconclusive (high Rm, low sterane and triaromatic steroid ratios), but by comparison to other oils we suggest BGR-1 was also likely generated in the peak oil window.

Grelowski and Czechowski (2011) noted that crude oils reservoirised in Ca2 facies in SW Poland (Gorzów Block located north of the Fore-Sudetic Monocline) have a higher maturity than Ca2 oils located in NW Poland. However, high maturity of PL-18 and -19 and to some extent PL-13 located in NW Poland suggests local high thermal maturity conditions. In the case of oils located in the TB, corresponding natural gases may indicate slightly higher maturities than in the other regions of Germany (Gerling et al., 1996a).

## *5.2. Palaeosetting during oil source rock deposition*

### *5.2.1 Stable carbon isotopes of hydrocarbon fractions*

$\delta^{13}\text{C}$  values of oils and oil fractions can be used for petroleum correlation (Peters et al., 2005), age classification (Andrusevich et al., 1998) or reconstruction of the depositional environment (Sofer, 1984; Chung et al., 1992).  $\delta^{13}\text{C}$  values of the saturated fraction of the studied oils vary between -30.6 and -24.3‰, whereas the aromatic fraction has  $\delta^{13}\text{C}$  values ranging from -31 to -23.9‰ (Fig. 5, Table 1). The canonical variable (CV=0.47; Sofer, 1984), which separates non-waxy (marine) and waxy (non-marine) oils, varies between -4.4 and 2.2. All signatures indicate that the source rocks for the studied oils were deposited in a marine setting. However, the BGR-4 oil falls slightly off the transition field between marine and terrigenous origin of oils, suggesting some contribution from terrigenous OM (CV = 2.2), but other biomarker signatures (e.g. homohopanes, steranes) strongly support predominantly marine OM.

Figure 5 shows several oil groupings (described in Section 6 in more detail); for example PL-4, -5, -12, -13 and -21 (NW Poland), occurring in Ca2 lower slope-shallow basin facies (Fig. 2), have the lowest  $\delta^{13}\text{C}$  values. Higher  $\delta^{13}\text{C}$  values are given by BGR-6, -7, -8 and -9, which make up another group of oils located in the TB and reservoir in lagoonal facies (Fig. 2). The highest  $\delta^{13}\text{C}$  values ( $\sim -26$  to  $-24$  ‰) are in BGR-12, -13, -14, PL-6 and -7 located in SE Germany and SW Poland, respectively, and occurring in lagoonal and inner shoal facies. Other oil groups, like PL-16, -18, -19 and -20, or BGR-4, rather reflect individual oil-fields which may have been sourced from a different type of OM. Stable carbon isotope ratios must be used with caution in indicating source input because of fractionations during and after formation of the OM. Therefore,  $\delta^{13}\text{C}$  isotopes should be used in tandem with other source- and age- diagnostic biomarkers which would allow more confident assessment of OM input (Peters et al., 2005). Nonetheless, Simoneit et al. (1993) also reported that  $\delta^{13}\text{C}$  values of Permian marine OM range from  $-31$  to  $-26$  ‰, which are almost entirely within the range for saturated and aromatic fractions of Ca2 oils, suggesting predominantly a common source of marine OM. The heaviest  $\delta^{13}\text{C}$  values in BGR-12, -13, -14, PL-6 and -7 suggest algal-rich OM that was probably deposited in a hypersaline environment (Table 1; Grice et al., 1998).

### 5.2.2 Water column stratification inferred from Ca2 oils

A suite of biomarkers was used to assess redox conditions and depositional environment during formation of source rocks for the investigated crude oils including the carbon preference index (CPI),  $\text{Pr}/n\text{-C}_{17}$  versus  $\text{Ph}/n\text{-C}_{18}$ , even-over-odd predominance (EOP) of  $n$ -alkanes,  $\text{C}_{31}\text{-C}_{35}$  homohopane distributions, the homohopane index (HHI) expressed as  $\text{C}_{35}/(\text{C}_{31}\text{-C}_{35})$  and  $\text{C}_{35}\text{S}/\text{C}_{34}\text{S}$ , the concentration of isorenieratene and chlorobactene derivatives, 28,30-bisnorhopane (BNH) abundance expressed as  $\text{BNH}/\text{C}_{30}\ 17\alpha\text{-hopane}$  (BNH/H), and gammacerane abundance expressed as  $\text{gammacerane}/\text{C}_{30}\ 17\alpha\text{-hopane}$  (G/H) (Table 1).

The calculated CPI for almost all oils is close to 1.0 (Table 1) but an EOP for the  $\text{C}_{20-30}$   $n$ -alkanes is observed in some oils (Fig. 6). An EOP is typical of biomass deposited in restricted marine carbonate/evaporite facies (Palacas et al., 1984; Mello et al., 1988a,b).

The patterns in the  $\text{Pr}/n\text{-C}_{17}$  versus  $\text{Ph}/n\text{-C}_{18}$  plot (Fig. 3; Table 1) indicate primary accumulation of marine OM under reducing conditions (Connan and Cassou, 1980; Palacas et al., 1988) for the source rocks of the Ca2 oils. However, these values can be thermally modified in oils of higher maturity (BGR-6, -7, -8, -9, PL-18, -19 and -24).

Homohopane distributions (Fig. 7) can be utilized to differentiate between oxic and reducing palaeodepositional environments, but the distributions can be affected by maturity and secondary alteration (Peters and Moldowan, 1991). The distribution for oils from NE Germany and NW Poland is characterised by elevated relative abundances of C<sub>35</sub> homohopanes indicating that Zechstein carbonate and evaporite facies were deposited in a restricted setting with anoxic bottom water (Boon et al., 1983; Connan et al., 1986; Fu et al., 1986; ten Haven et al., 1988; Mello et al., 1988a,b; Clark and Philp, 1989; Słowakiewicz et al., 2015, 2016a); such conditions have been interpreted to be accompanied by the presence of reduced sulphur species in the water column (ten Haven et al., 1988; Sinninghe Damsté et al., 1995a). The reducing depositional conditions are also expressed by high HHIs (0.12-0.31, average 0.2) and C<sub>35</sub>S/C<sub>34</sub>S (0.39-1.71) (Table 1). High HHIs in oil samples from NE Germany and NW Poland correspond well to high HHIs (0.12-0.56) reported predominantly from the Ca2 lower slope facies of the northeastern margin of the SPB (Słowakiewicz et al., 2016a). Oils from SE Germany and SW Poland have lower HHIs (0.12-0.18) and C<sub>35</sub>S/C<sub>34</sub>S (0.74-1.05) (Table 1) suggesting suboxic/anoxic conditions consistent with relatively low HHIs (0.03-0.17[4], average 0.04-0.09) found in lagoonal facies (Słowakiewicz et al., 2016a).

All oil samples are characterised by the dominance of C<sub>30</sub> 17 $\alpha$ -hopane over lower or higher homologues in many oil samples (Fig. 6). The majority of oil samples have elevated abundances of C<sub>32</sub> and C<sub>34</sub> hopanes (particularly oils from S Germany, Fig. 6, 7), which are believed to indicate suboxic (high C<sub>32</sub>)/anoxic (high C<sub>34</sub>) source-rock depositional environments (Peters and Moldowan, 1991). In addition, the dominance of 17 $\alpha$ -C<sub>34</sub> over C<sub>33</sub> and C<sub>35</sub> homologues indicates a carbonate lagoonal and evaporitic environment source (Waples and Machihara, 1991) or suggests an unknown source of bacteriohopanepolyols. BGR-9, PL-18, -19, -24 contain lower abundances or an absence of C<sub>31</sub>-C<sub>35</sub> homohopanes, likely due to thermal degradation during catagenesis (Table 1).

Biomarkers for anaerobic phototrophic green sulphur bacteria provide strong constraints on the redox state and water column stratification indicating PZE during source rock deposition (Summons and Powell, 1986; Sinninghe Damsté et al., 1993). Isorenieratane,  $\beta$ -isorenieratane, C<sub>14-31</sub> 2,3,6-aryl isoprenoids, and chlorobactane are present in most of the oils (Fig. 6, Table 1); they were not detected in BGR-13, PL-4, -5, -12, -13, -18, -19, -21, and -24. Concentrations of isorenieratane and chlorobactane vary between 16 and 710  $\mu\text{g g}^{-1}$  oil and 1 and 65  $\mu\text{g g}^{-1}$  oil, respectively. The overall highest concentrations of isorenieratene derivatives in our dataset occurred in oils from NE Germany and NW Poland (isorenieratane:

22-710  $\mu\text{g g}^{-1}$  oil, chlorobactane: 3-65  $\mu\text{g g}^{-1}$  oil, presence of  $\beta$ -isorenieratane; Fig. 6, Table 1).

Intriguingly, PL-12 and -21 oils, which do not contain isorenieratane and chlorobactane and were derived from the Ca2 lower slope facies, may mark the maximum basinward extent of PZE as it impinged on the NE slope of the SPB (Fig. 2a). Therefore, of all Ca2 oil biomarkers, the C<sub>40</sub> carotenoids (isorenieratene derivatives) seem to be particularly important for Ca2 oils and source rocks. However, isorenieratene derivatives also occur in the Kimmeridge Clay Formation (e.g., van Kaam-Peters et al., 1988) and Oxford Clay Formation (Kenig et al., 2004), even though both are only regarded as source rocks for petroleum in the central and northern North Sea and are insignificant in the southern North Sea (Lott et al., 2010). They also occur in the Posidonia Shale Formation (Frimmel et al., 2004), important only in the Dutch rift basins and in Germany (Lott et al., 2010), in Devonian black shales (Joachimski et al., 2001) with no petroleum generation potential reported (Pletsch et al., 2010), Oligocene Menilite beds in the Polish and Ukrainian Carpathians (Kotarba et al., 2007) being the most important source rock for the Carpathian Province (Curtis et al., 2004, Kotarba and Koltun, 2006) and in Middle Rhaetian shales in Germany (Blumenberg et al., 2016). Consequently, French et al. (2015) concluded that in addition to PZE, other factors, such as an origin from microbial mats, an allochthonous input, planktonic origin or production of these biomarkers in ‘no analogue’ palaeoenvironments, should be taken into account to explain sources of isorenieratene derivatives.

Similarly, Słowakiewicz et al. (2015, 2016) only found isorenieratene derivatives in the shallow basin and lower slope facies and in lagoons of the northeastern and southern SPB. Reducing and even euxinic conditions likely existed in restricted lagoons dominated by production of microbialites under high salinity conditions, but isorenieratane and chlorobactane have not been detected in oolite shoal facies on the northeastern SPB, excluding redeposition of isorenieratene derivatives into subtidal settings of the Ca2 carbonate platform. However, the presence of isorenieratane and chlorobactane in lagoons and inner oolite shoals of the southern SPB suggests that such settings were their source in some Ca2 oils (i.e., BGR-12, -14, PL-10, -14, -16, -17, -20).

Anoxic conditions during deposition of source rocks are also confirmed by the occurrence of BNH detected in some oils (Table 1). BNH is a desmethylhopane of unknown origin but generally regarded as indicative of anoxic or euxinic deposition (e.g. Curiale et al., 1985;

Mello et al., 1990; Peters et al., 2005). The BNH/H ratio can be applied as a facies parameter, provided that the oil samples are not of too high maturity. BNH was detected in all oils from Poland (except for PL-3) and the BNH/H ratio in the Polish oils varies between 0.01 and 0.21. Abundant BNH in PL-18 and -19 indicates deposition of the source rock under clay-poor anoxic conditions (Katz and Elrod, 1983; Mello et al., 1988a; Curiale and Odermatt, 1989). Alternatively, the ratio may be affected by maturity as the relative amount of BNH can decline with increasing maturity (Peters et al., 2005). BNH (BNH/H 0.1 – 0.24) was also detected in the lowermost lower slope and shallow basin facies in the Ca2 on the northern margin of the eastern SPB (NW Poland, Słowakiewicz et al., 2015) which would suggest a common source for oils located in NW Poland. However, BNH was not detected in core samples from other parts of the SPB (Słowakiewicz et al., 2015). Nevertheless, its absence, also in oil samples from Germany and PL-3, does not preclude sedimentation under anoxic conditions.

Gammacerane, which is also present in the studied oils, is commonly invoked as additional evidence for a stratified water column in marine and non-marine depositional environments and/or specifically for hypersalinity (Moldowan et al., 1985; Jiamo et al., 1986; Sinninghe Damsté et al., 1995b). Gammacerane is believed to derive from tetrahymanol, which is produced by ciliates feeding on bacteria at oxic-anoxic transition zones. The abundance of gammacerane, expressed as G/H ratios (Sinninghe Damsté et al., 1995b), varies from 0.09 to 0.41 (Table 1). This may indicate slightly elevated salinity conditions during source rock deposition and corresponds to G/H (0.1-0.6) obtained from lower slope-shallow-basin and hypersaline lagoonal Ca2 facies (Słowakiewicz et al., 2015, 2016a). Gammacerane was not detected in BGR-9, PL-18 and -19.

In summary, our data suggest that Ca2 oils were generated from source rocks deposited under suboxic-anoxic(euxinic) marine carbonate-evaporite conditions with various strengths of water column stratification as evidenced by e.g., G/H. Gammacerane most commonly occurs in high abundance in the more restricted portions of the Ca2 basin and in restricted/hypersaline lagoons (Słowakiewicz et al., 2016a). Specifically, gammacerane abundance, which mirrors that of BNH, was detected in the lowermost sections of the lower slope facies and in the shallow-basin facies (NE margin of the Ca2 sea). It was interpreted as a record of marine hypersalinity during the early stage of the Ca2 transgression and carbonate precipitation as a part of the carbonate-evaporite cycle (Słowakiewicz et al., 2015), which additionally could support a carbonate-evaporite source for the Ca2 oils.

### 5.3. Source of organic matter

The tricyclic/17 $\alpha$ -hopane ratio can be used for assessment of thermal maturity of oils (Seifert and Moldowan, 1978), but it is commonly applied in the identification of the principal source rocks (Peters et al., 2005). The tricyclic/17 $\alpha$ -hopane ratio in the majority of oil samples is 0.03-0.53 (average 0.16, standard deviation [SD] 0.14) and in two samples (BGR-7 and -9) is >1 (Table 1). High (>1) tricyclic/17 $\alpha$ -hopane ratios can be attributed to marine depositional conditions rather than maturity (Seifert and Moldowan, 1979; Philp et al., 1992). However, da Cruz et al. (2011) noted that oils with lower tricyclic/17 $\alpha$ -hopane ratios, usually interpreted as more mature oils, could be the consequence of anaerobic microbiota degradation operating at higher temperatures. Regardless, a moderately high tricyclic/17 $\alpha$ -hopane ratio in tandem with high G/H and HHIs is consistent with deposition in a high-salinity marine environment.

The source rock for Ca2 oils can also be explored using the C<sub>21</sub>/C<sub>22</sub> and C<sub>24</sub>/C<sub>23</sub> tricyclic terpane ratios (in general, high C<sub>21</sub>/C<sub>22</sub> and low C<sub>24</sub>/C<sub>23</sub> occur in oils derived from carbonate source rocks; Zumberge et al., 2005), the C<sub>19</sub>/C<sub>21</sub> tricyclic and C<sub>24</sub> tetracyclic (Tet)/C<sub>23</sub> tricyclic terpane ratios (abundant C<sub>24</sub> tetracyclic terpane in oils indicates carbonate or evaporite source rocks, Palacas et al., 1984; Connan et al., 1986; Connan and Dessort, 1987; Clark and Philp, 1989; or abundant tricyclic and tetracyclic terpanes can indicate high thermal maturity, Farrimond et al., 1999), as well as the C<sub>29</sub> 17 $\alpha$ -norhopane/C<sub>30</sub> 17 $\alpha$ -hopane ratio (C<sub>29</sub>/H, high [>0.8] in oils derived from anoxic carbonate or marl source rocks; Palacas et al., 1984; Clark and Philp, 1989).

For these oils, the C<sub>21</sub>/C<sub>22</sub> and C<sub>24</sub>/C<sub>23</sub> tricyclic terpane ratios suggest a marly carbonate-evaporite depositional environment for Ca2 oils (Fig. 8). Similarly, the C<sub>19</sub>/C<sub>21</sub> tricyclic and C<sub>24</sub> Tet/C<sub>23</sub> tricyclic terpane ratio indicates that Ca2 oil groups are facies-controlled rather than maturity-controlled and high C<sub>24</sub> Tet values imply a carbonate-evaporite depositional environment for the source rocks (Fig. 9, Table 1). The C<sub>29</sub>/H ratio, which ranges from 0.3 to 5.8, suggests terrigenous-carbonate/marl-type of OM, but the highest values (>2) could be thermally controlled (Table 1).

The diasterane/sterane ratio expressed as C<sub>29</sub> 13 $\beta$ ,17 $\alpha$ (H) (20S + 20R)/(C<sub>29</sub> 5 $\alpha$ ,14 $\alpha$ ,17 $\alpha$ (H) 20S + 20R + 5 $\alpha$ ,14 $\beta$ ,17 $\beta$ (H) 20S + 20R) also helps to distinguish oils from carbonate versus clastic source rocks (Mello et al., 1988a). High diasterane/sterane ratios are typically interpreted to derive from clay-rich source rocks but high ratios have also been

observed in extracts from organic-lean and clay-poor carbonate rocks (Palacas et al., 1984; Moldowan et al., 1991), although high ratios in oils can also result from high thermal maturity or heavy biodegradation (Seifert and Moldowan, 1978, 1979). Van Kaam-Peters et al. (1998) observed that the diasterane/sterane ratio does not correlate with clay content but depends on the amount of clay relative to the amount of OM which can explain high diasterane/sterane ratios in oils derived from carbonate source rocks. The diasterane/sterane ratio in the majority of oil samples varies between 0.04 and 0.8 suggesting carbonate-evaporite source rocks with an abundant clay (marl) content (Table 1). The Pr/Ph versus C<sub>27</sub> diasteranes / (diasteranes + regular steranes) plot also suggests a carbonate-evaporite depositional environment for the Ca2 oils' source rocks (Fig. 10). Very high diasterane/sterane ratios in PL-18, -19 and -24 (~2-3) can result from high thermal maturity (see Fig. 4 and Section 5.1, Seifert and Moldowan, 1978; van Graas, 1990), which is also confirmed by the reduced homohopane distributions, rendering the sterane data difficult to interpret in terms of OM source for those oils.

The dibenzothiophene/phenanthrene (DBT/P) ratio can also indicate source rock lithology, with carbonate rocks having ratios >1 and shales having ratios <1 (Hughes et al., 1995). In addition, high DBT/P ratios indicate the incorporation of reduced sulphur into OM in the source rocks, typical of carbonate-evaporite environments (Hughes et al., 1995). Accordingly, the source rock for oils in NE and SE Germany and BGR-9 contained relatively more clay/marl or evaporite (high C<sub>24</sub>/C<sub>23</sub> 0.65 – 0.99) (Fig. 8), than carbonate indications (C<sub>29</sub>/H 0.37 – 0.68, DBT/P 0.09 – 1.18; Fig. 11; Table 1). In other oils the proportion of evaporite/clay decreases at the expense of marl/carbonate. However, Figure 11 and Table 1 show that the DBT/P ratio in PL-18 and -19 is very high (>13), which is likely thermally affected, and thus the obtained values cannot be reliably interpreted with respect to depositional setting. However, they can serve as reliable high-maturity indicators.

The Ca2 oils include abundant C<sub>27</sub>-C<sub>29</sub> 4-desmethyl steranes, with C<sub>29</sub> steranes being more abundant than the total C<sub>27</sub>-C<sub>28</sub> steranes in 13 oil samples (Table 1, Fig. 12). The regular sterane distribution is consistent with either terrigenous or marine algal OM (Huang and Meinschein, 1979; Volkman, 1986; Volkman et al., 1998; Kodner et al., 2008), but is mostly indicative of algal-dominated carbonate marine settings (Palacas et al., 1984; Walter and Cassa, 1985; Grantham, 1986). The C<sub>27</sub>/C<sub>29</sub> and C<sub>28</sub>/C<sub>29</sub> sterane ratios in almost all samples vary from 0.3 to 1.7 and 0.3 to 0.9, respectively (Table 1). The highest of these sterane ratios are in PL-18 and -19 (Table 1, Fig. 12), and they are likely thermally controlled

and should be treated with caution. It also should be noted that a high-maturity interpretation for these samples is consistent with the high DBT/P and Ts/Tm versus C<sub>27</sub> diasteranes/(diasteranes + regular steranes) ratios which also appear to be maturity-induced. In some cases, the C<sub>27</sub>/C<sub>29</sub> ratio can be used to indicate the relative inputs of algae relative to higher plants based on the dominance of C<sub>29</sub> steroids in the latter (Huang and Meinschein, 1979); however, many algae also synthesize C<sub>29</sub> sterols (Volkman, 1986; Volkman et al., 1998; Kodner et al., 2008). Although the C<sub>27</sub>/C<sub>29</sub> sterane ratio is typically >1 in marine-dominated depositional systems (Grantham and Wakefield, 1988), lower ratios are typical for predominantly marine Permian/Triassic sections (Cao et al., 2009; Hays et al., 2012; Słowakiewicz et al., 2015, 2016a).

The C<sub>28</sub>/C<sub>29</sub> sterane ratio has been used to distinguish Upper Cretaceous and Cenozoic oil from Palaeozoic or older oil (Grantham and Wakefield, 1988). These authors observed that the C<sub>28</sub>/C<sub>29</sub> sterane ratios for crude oils from marine source rocks with little or no terrigenous OM input are <0.5 for lower Palaeozoic and older oils, 0.4-0.7 for upper Palaeozoic to Lower Jurassic oils, and greater than approximately 0.7 for Upper Jurassic to Miocene oils. Earlier than the Mesozoic, however, C<sub>28</sub> steranes were also likely derived from green algae, particularly prasinophytes (Kodner et al., 2008). It is also important to note that Słowakiewicz et al. (2016a) attributed the C<sub>28</sub>/C<sub>29</sub> sterane ratio variability to basin-scale differences in algal ecology. Therefore, we interpret the C<sub>28</sub>/C<sub>29</sub> sterane ratios (0.31 to 1.42, average ~0.47, excluding PL-18 and -19) as resulting from the proportion between C<sub>29</sub> sterane-producing green algal groups and C<sub>28</sub> sterane-producing red and prasinophyte algae (Kodner et al., 2008) in carbonate-evaporite environments. Thus, we conclude that the C<sub>28</sub>/C<sub>29</sub> sterane ratios in our sample set suggest significant input of green algae to the total biomass.

The regular steranes/17 $\alpha$ -hopanes ratio is commonly used to reflect input of algae and higher plants versus bacteria, but increasing maturity elevates this ratio (Seifert and Moldowan, 1978; Requejo, 1994). The steranes/17 $\alpha$ -hopanes ratio (0.1-2, Table 1) in our oil samples suggests a high proportion of algae to bacteria (average 0.55), yet some values in BGR-9, PL-18, -19 and -24 may result from high thermal maturity.

In summary, Ca2 oils were derived from a source rock whose OM contained various proportions of algae and bacteria and to a much lesser degree terrestrial plants depending on the type of the carbonate/evaporite depositional environment.



## 483           **6. Implications for the inferred source of Ca2 oils and oil grouping**

484           The Ca2 oil samples were derived from marine source rocks and the calculated CV (Table  
485 1) classifies almost all Ca2 oils as non-waxy ( $CV < 0.47$ ). The biomarker parameters show that  
486 Ca2 oils were predominantly derived from mixed sulphate(+clay)-carbonate or marly  
487 carbonate lithofacies, i.e., the Ca2 source rocks as well as overlying and underlying  
488 anhydrites.

489           Collectively, the biomarker data presented here show the characteristic lipid biomarkers  
490 which can be applied in correlating Ca2 oils from shallow basin-lower slope and lagoonal-  
491 oolite shoal carbonate facies, located in the NE, SE and S SPB (Fig. 2). The marly carbonate  
492 source rocks are characterized by a significant contribution of sapropelic (algal + microbial)  
493 and subordinate clay(marl)-associated OM and they are chiefly located in lower  
494 slope/shallow-basin and lagoonal facies. The presence of clay minerals in the Ca2 carbonate  
495 matrix has also been noted by Schwark et al. (1998) and Grelowski and Czechowski (2011)  
496 and this is reflected by the increased abundance of diasteranes in the Ca2 oils. Generally,  
497 evaporite (anhydrite) rocks containing clays (e.g., chicken-wire anhydrite), but also marl and  
498 micritic limestone deposited under anoxic conditions, have long been considered as important  
499 source rocks for hydrocarbons (Kirkland and Evans, 1981; Sonnenfeld, 1985; Jiamo et al.,  
500 1986; Warren, 1986, 2011; Bousson, 1991; Edgell, 1991). The marginal and  
501 subaerial/shallow-water upper part of Z1 (Upper Anhydrite or Werra Anhydrite = Lower +  
502 Upper Anhydrite) and Z2 (Basal Anhydrite) anhydrite (Fig. 2) contains bituminous  
503 carbonate-anhydrite laminites and chicken-wire anhydrite (Taylor, 1998; Słowakiewicz and  
504 Mikołajewski, 2009; Peryt et al., 2010), which could have been an additional source for Ca2  
505 oils. In addition, anhydrite is an important contributor to the Ca2 hypersaline lagoonal facies  
506 and interbeds with the Ca2 facies which would explain the evaporitic nature of the Ca2 oils  
507 studied and hence their additional sulphate-type OM source.

508           Ca2 oils share characteristic biomarker ratios which also are specific to particular SPB  
509 areas. Thus, they can be distinguished from oils generated from other source rocks and time  
510 intervals. The characteristic biomarkers of many Ca2 oils include: a) CPI ~1 and an EOP in  
511 the range of  $C_{20-30}$  *n*-alkanes characteristic of carbonate/evaporite source rocks deposited in  
512 hypersaline settings; b)  $C_{40}$  carotenoids (isorenieratane (0)16-709  $\mu\text{g g}^{-1}$  oil, chlorobactane  
513 (0)1-65  $\mu\text{g g}^{-1}$  oil,  $\beta$ -isorenieratane), although these are only characteristic for oils reservoired

in (and most likely sourced from) shallow-basin to lower slope and lagoonal facies and are characteristic of oils located in NE Germany and NW Poland; c) 28,30-bisnorhopane (BNH/H 0.01-0.07) occurs in oils from the shallow-basin/lower slope-lagoonal facies in NW and SW Poland; d) high abundance of C<sub>35</sub> homohopanes was detected in oils from shallow-basin/lower slope-lagoonal facies in NW Poland and NE Germany; e) a predominance of C<sub>34</sub> homohopanes over C<sub>33</sub> and C<sub>35</sub> homohopane homologues occurs in oils from lagoonal facies in the TB; f) the majority of Ca2 oils have C<sub>29</sub> steranes dominant over C<sub>27</sub> and C<sub>28</sub> homologues but that is interpreted as deriving from a green algal marine, rather than terrestrial, OM source; g) a high abundance of diasteranes relative to regular steranes (>0.1) in almost all Ca2 oils is typical of petroleum derived from source rocks with an abundant clay content; h) very high BNH/H (~0.2), Ts/Tm (>10), C<sub>29</sub>/H (>4), DBT/P (>13) ratios are characteristic of PL-18 and -19 suggesting relatively high thermal maturity and clay-poor carbonate source rocks deposited under anoxic conditions. These suggested Ca2 characteristic oil biomarkers correlate well with their analogues detected in Ca2 rock extracts (Słowakiewicz, 2016), whereas the correlation for BGR-9, PL-18, -19 and -24 with potential source rocks could not be reliably determined, probably due to elevated maturity levels. Despite these general characteristics of Ca2 oils, based on  $\delta^{13}\text{C}$  isotopes, homohopane distributions, sterane ratios, isorenieratene derivatives, as well as regional occurrences and previous interpretations on the local facies, the following oil sample classification is suggested:

**Group 1:** BGR-12, -13, -14, PL-6 and 7 located in SE Germany and SW Poland and reservoired in inner shoal (BGR-13, PL-6, -7) and lagoonal facies (BGR-12, -14). They are characterised by the heaviest  $\delta^{13}\text{C}$  isotopes (-24 to -26 ‰) and were derived from algal-rich carbonate-evaporite source rocks deposited under anoxic (euxinic) conditions in Ca2 hypersaline lagoons. They are also characterised by slightly elevated C<sub>34</sub> homohopanes (except for BGR-14, Fig. 7).

**Group 2:** BGR-1, -2, -3 and -4 are reservoired in lower slope facies.  $\delta^{13}\text{C}$  isotopes vary between -27 and ~-25 ‰. The oils derived from predominantly algal (high sterane/17 $\alpha$ -hopane ratios) carbonate/evaporite Ca2 lower slope source rocks deposited under reducing (HHI 0.19-0.23), euxinic (isorenieratane 159-408  $\mu\text{g g}^{-1}$  oil, chlorobactane 27-65  $\mu\text{g g}^{-1}$  oil) and hypersaline conditions (G/H 0.16 to 0.19). They are characterised by abundant concentrations of C<sub>35</sub> homohopanes (Fig. 7).

**Group 3:** PL-1, -2, -3, -8, -9, -11, -15, -22, -23 are reservoired in lower slope and lagoonal/oolite shoal facies.  $\delta^{13}\text{C}$  isotopes vary between  $\sim -27$  and  $\sim -26$  ‰. Group 3 is similar to Group 2 oils but were derived from predominantly microbial-algal carbonate/evaporite Ca2 lower slope/lagoonal source rocks. Group 3 is characterised by the highest HHI (0.2-0.3),  $\text{C}_{35}\text{S}/\text{C}_{34}\text{S}$  and G/H (0.2-0.35) ratios, and isorenieratane (23-709  $\mu\text{g g}^{-1}$  oil) and chlorobactane ([0]3-53  $\mu\text{g g}^{-1}$  oil) concentrations. They are also characterised by abundant  $\text{C}_{35}$  homohopanes (Fig. 7).

**Group 4:** BGR-5 (NE Germany) and BGR-10, -11 and -15 located in SE Germany are all reservoired in outer shoal facies.  $\delta^{13}\text{C}$  isotopes vary between  $-26$  and  $\sim -28$  ‰. The oils were derived from algal-rich (the highest sterane/ $17\alpha$ -hopane ratios), carbonate/evaporite Ca2 lagoonal source rocks deposited under slightly reducing (HHI 0.12-0.16), euxinic (isorenieratane 125-360  $\mu\text{g g}^{-1}$  oil, chlorobactane 17-47  $\mu\text{g g}^{-1}$  oil) and hypersaline conditions (G/H 0.09-0.11). They are characterised by elevated  $\text{C}_{34}$  homohopanes (Fig. 7).

**Group 5:** PL-16 and -20 located in SW Poland are reservoired in shallow-basin (PL-20) facies. This group is similar to Group 3 but has slightly elevated  $\text{C}_{34}$  homohopanes, abundant  $\text{C}_{27}$  steranes, lacks elevated  $\text{C}_{35}$  homohopanes (Fig. 7), and was deposited in reducing (HHI 0.17, BNH 0.06), euxinic (isorenieratane 46-50  $\mu\text{g g}^{-1}$  oil) and hypersaline (G/H 0.23-0.27) conditions. Additionally, relatively low abundance of isorenieratene derivatives may suggest temporary euxinia and less restricted depositional conditions. PL-16 and -20 are derived from algal-rich carbonate/evaporite source rocks likely located in Ca2 shallow-basin facies.

**Group 6:** BGR-9 and PL-24 oils are reservoired in oolite (BGR-9) and shallow-marine dolo- and lime- mudstone (PL-24) facies. High thermal maturity evidenced by the high  $\text{Ts}/\text{Tm}$  (5.2-9.2, Table 2) and  $\text{C}_{29}/\text{H}$  (0.8-2) ratios, the low abundance of hopanes and absence of isorenieratane or chlorobactane precludes a reliable interpretation of the OM source for these oils. However, high  $\text{C}_{24}\text{Tet}/\text{C}_{23}$  values might suggest a carbonate-evaporite depositional environment for the source rocks.

**Group 7:** PL-18 and -19 are reservoired in outer oolite facies of the Pomeranian carbonate platform (Fig. 2a). Thermal maturity is high (Table 2), similar to Group 6. High thermal maturity is supported by very high  $\text{Ts}/\text{Tm}$  (10.9-11.8, Table 2), diasterane/sterane (2.99-3.02),  $\text{C}_{29}/\text{H}$  (4.36-5.78), DBT/P (13.2-14.5, Fig. 9) and BNH/H (11-12) ratios. The  $\text{C}_{24}/\text{C}_{23}$  (0.78-0.85) tricyclic ratio and high  $\text{C}_{24}\text{Tet}/\text{C}_{23}$  values could indicate a carbonate/evaporite source rock.

**Group 8:** BGR-6, -7, and -8 occur in the southwest TB in lagoonal facies.  $\delta^{13}\text{C}$  isotopes vary between -29 and -28 ‰. The oils were derived from algal-rich (high  $\text{C}_{27}/\text{C}_{29}$  sterane ratios) clay/marl or evaporite, rather than carbonate, deposited in Ca2 lagoonal facies under slightly reducing (HHI 0.13-0.14) and hypersaline depositional conditions (G/H 0.16 to 0.17).  $\text{C}_{15}$  to  $\text{C}_{31}$  2,3,6-aryl isoprenoids are present and isorenieratane – if at all – occurs only in traces, which might be the result of relatively high thermal maturity (Table 2; Summons and Powell, 1986). Elevated concentrations of  $\text{C}_{34}$  homohopanes over  $\text{C}_{33}$  and  $\text{C}_{35}$  homologues are characteristic of the Group 8 oils.

**Group 9:** PL-4, -5, -12, -13 and 21 occur in NW Poland in lower slope/shallow-basin facies. They are characterised by the lightest  $\delta^{13}\text{C}$  isotopes (~-31 and -30 ‰). The source rock for Group 9 received more clay/marl or evaporite than carbonate input, along with a significant algal source (abundant  $\text{C}_{27}$  steranes) located in Ca2 lower slope/shallow-basin facies deposited under reducing and hypersaline conditions. Chlorobactane, isorenieratane or  $\beta$ -isorenieratane were not detected (Fig. 6). Elevated concentrations of  $\text{C}_{32}$  and  $\text{C}_{35}$  homohopanes over lower and higher homologues are characteristic of this group. PL-4 and -5 oils, which are reservoirised in Ca3 basin (dolo-mudstone and anhydrite) facies, have biomarker characteristics similar to Ca2 oils in this group which suggests that Ca3 oils may have been generated and migrated from Ca2 lower slope/shallow-basin facies.

**Group 10:** PL-10, -14, -17 occur in SW Poland in inner shoal/lagoonal facies. They are similar to Group 1 but have less depleted  $\delta^{13}\text{C}$  isotopes (-26.6 to -25.6 ‰). Group 10 is characterised by an almost even percentage of  $\text{C}_{33-35}$  homohopanes. The oils were derived from microbial-rich source rocks deposited under anoxic/euxinic (HHI 0.16-0.18, BNH/H 0.02-0.05, isorenieratane 141-341  $\mu\text{g g}^{-1}$  oil, chlorobactane 6-14  $\mu\text{g g}^{-1}$  oil) conditions in Ca2 hypersaline lagoons.

## 7. Conclusions

As is the case for petroleum systems in general, Zechstein reservoirs are heterogeneous and an in-depth understanding would be possible only after detailed examination of a much larger dataset. Such attempts were beyond the scope of this paper and, furthermore, complete datasets on the individual systems were not available. However, from the available dataset we have integrated a suite of various biomarker parameters in order to interpret redox conditions

and OM source for Ca2 oils. Thirty-nine Zechstein Main Dolomite oils were analysed to investigate their origin in the eastern and south-central sector of the Southern Permian Basin of Europe. The investigated Ca2 oil samples reveal 10 groups based on their stable carbon isotopes, biomarker fingerprints and subtle biomarker differences. The oils show strong geochemical similarity within these particular groups and in some cases, sharp differences among them. The thermal maturity of the studied oils corresponds to the peak to late oil window, the latter being difficult to interpret with respect to source.

The biomarker correlations between the Ca2 oils revealed that the very high DBT/P and sterane ratios can be used for thermal maturity assessments for Zechstein Main Dolomite oils. With respect to source, these biomarker data indicate that the oils were derived from evaporite- and carbonate- rich source rocks (i.e., the Main Dolomite and overlying and underlying evaporites) deposited under marine conditions and characterized by a significant contribution of sapropelic (algal + microbial) OM and a subordinate clay(marl)-associated OM. Source rocks for Groups 6 and 7 oils could not be clearly determined due to their high thermal maturity and low abundance of source-specific biomarkers, although high C<sub>24</sub>Tet/C<sub>23</sub> values suggest a carbonate-evaporite depositional environment for their source rocks as well. Importantly, some characteristic biomarkers allowed more nuanced identification of source facies; for example, C<sub>40</sub> aromatic carotenoids are particularly distinct among oils, and isorenieratene derivatives were used for oil groupings, for the first time to the best of our knowledge. Collectively, this allowed the identification of the 10 distinct groups, defined by depositional environment, geographical location in the SPB, OM source and thermal maturity.

## Acknowledgements

We dedicate this paper to the memory of Dr Cezary Grelowski (†), an excellent petroleum geochemist. After finishing his studies he worked in the Piła Branch of the Polish Oil and Gas Company (PGNiG SA) for the rest of his life. Being fascinated with his work and new geochemical concepts, Cezary was a fantastic partner in the field and laboratory. Having a predisposition to scientific work he would approach difficult problems with unconventionally disputing the erudition and profound knowledge of the matter. Dr Cezary Grelowski was a cordial, obliging, friendly person, and remained an optimist, never despairing in his work on his passion – organic geochemistry! His credo was knowledge, hard work and helpfulness, till the end, and as such a person he will remain in our memory.

We also dedicate this paper to Dr Franz Kockel (†), for his outstanding and successful engagement for developing collaboration between geoscientists from the Central European Basin area. Understanding geology is only possible in a holistic way – a basic principle exemplified by Franz Kockel. It was his heartfelt wish to share his experience in regional geology with colleagues from neighbouring countries, especially from Central Europe.

Some crude oil samples (Poland) were kindly obtained from GeoMark Research (Houston). Shell Exploration and Production is thanked for partial financial support and ENGIE for permission to publish the results. The study of some Polish oils has also been financially supported by a statutory research project (no. 11.11.140.626) granted by the AGH University of Science and Technology, Kraków. We thank Jürgen Poggenburg for discussion, Monika Weiß, Adam Kowalski, James Williams and Alison Kuhl for help with instruments. We also wish to thank the Natural Environment Research Council (NERC), UK, for partial funding of the mass spectrometry facilities at Bristol (contract no. R8/H10/63). Finally, we acknowledge constructive and helpful comments of an associate editor Barry J. Katz, Benedikt Lerch, Joseph Curiale and two anonymous reviewers, which improved the quality of our manuscript. M.S. was supported by a Mobility Plus programme post-doctoral fellowship of the Ministry of Science and Higher Education of Poland and Shell Exploration and Production. R.D.P. acknowledges the Royal Society Wolfson Research Merit Award (UK).

## References

- Albrecht, H., 1932. Die Erdöllagerstätte Volkenroda. Zeitschrift der Deutschen Geologischen Gesellschaft 84, 361-363.
- Andrusevich, V.E., Engel. M.H., Zumberge, J.E., Brothers, L.A., 1998. Secular episodic changes in stable carbon isotope composition of crude oils. Chemical Geology 152, 59-72.
- Beach, F., Peakman, T.M., Abbott, G.D., Sleeman, R., Maxwell, J.R., 1989. Laboratory thermal alteration of triaromatic steroid hydrocarbons. Organic Geochemistry 14, 109-111.
- Best, G., 1989. Die Grenze Zechstein/Buntsandstein in Nordwest-Deutschland nach Bohrlochmessungen. Zeitschrift der Deutschen Gesellschaft für Geowissenschaften 147, 455-464.

- Blumenberg, M., Heunisch, C., Lückge, A., Scheeder, G., Wiese, F., 2016. Photic zone euxinia in the central Rhaetian Sea prior the Triassic-Jurassic boundary. *Palaeogeography, Palaeoclimatology, Palaeoecology* 461, 55-64.
- Boon, J.J., Hine, S.H., Burlingame, A.L., Klok, J., Rijpstra, W.I.C., de Leeuw, J.W., Edmunds, K.E., Eglinton, G., 1983. Organic geochemical studies of Solar Lake laminated cyanobacterial mats. In: Bjorøy, M., Albrecht, K., Cornford, K., de Groot, G., Eglinton, G., Galimov, E., Leythaeuser, D., Pelet, R., Rullkötter, J., Speers, G. (Eds.), *Advances in Organic Geochemistry 1981*. John Wiley & Sons, New York, pp. 207-227.
- Bousson, G., 1991. Relationship between different types of evaporitic deposits, and the occurrence of organic-rich layers (potential source-rocks). *Carbonate and Evaporites* 6, 177-192.
- Brosin, H. 2013. Die Erdölgewinnung in Thüringen - Von Anfang des 20. Jahrhunderts bis in die 1970er Jahre. Sonderheft der Beiträge zur Geologie von Thüringen, 154 pp.
- Cao, C., Love, G.D., Hays, L.E., Wang, W., Shen, S., Summons, R.E., 2009. Biogeochemical evidence for euxinic oceans and ecological disturbance presaging the end-Permian mass extinction event. *Earth and Planetary Science Letters* 281, 188-201.
- Chung, H.M., Rooney, M.A., Toon, M.B., Claypool, G.E., 1992. Carbon isotope composition of marine crude oils. *AAPG Bulletin* 76, 1000-1007.
- Clark, J.P., Philp, R.P., 1989. Geochemical characterization of evaporite and carbonate depositional environments and correlation of associated crude oils in the Black Creek basin, Alberta. *Bulletin of Canadian Petroleum Geology* 37, 401-416.
- Connan, J., Cassou, A.M., 1980. Properties of gases and petroleum liquids derived from terrestrial kerogen at various maturation levels. *Geochimica et Cosmochimica Acta* 44, 1-23.
- Connan, J., Bouroullec, J., Dessort, D., Albrecht, P., 1986. The microbial input in carbonate-anhydrite facies of a sabkha palaeoenvironment from Guatemala: a molecular approach. *Organic Geochemistry* 10, 29-50.
- Connan, J., Dessort, D., 1987. Novel family of hexacyclic hopanoid alkanes (C<sub>32</sub>-C<sub>35</sub>) occurring in sediments and oils from anoxic palaeoenvironments. *Organic Geochemistry* 11, 103-113.
- Curiale, J.A., Cameron, D., Davis, D.V., 1985. Biological marker distribution and significance in oils and rocks of the Monterey Formation, California. *Geochimica et Cosmochimica Acta* 49, 271-288.

- Curiale, J.A., Odermatt, J.R., 1989. Short-term biomarker variability in the Monterey Formation, Santa Maria Basin. *Organic Geochemistry* 14, 1-13.
- Curtis, J.B., Kotarba, M.J., Lewan, M.D., Więclaw, D., 2004. Oil/source rock correlations in the Polish Flysch Carpathians and Mesozoic basement and organic facies of the Oligocene Menilite Shales: insights from hydrous pyrolysis experiments. *Organic Geochemistry* 35, 1573-1596.
- Czechowski, F., Piela, J., 1997. Skład molekularny substancji organicznej zawartej w dolomicie głównym oraz skałach wylewnych z otworu Namyslin-1. *Nafta-Gaz* 53, 299-308.
- Czechowski, F., Piela, J., Grelowski, C., Hojniak, M., Wojtkowiak, Z., Pikulski, L., 1998. Geochemiczne przesłanki ciągłości złoża gazu i ropy naftowej w rejonie Barnówko-Lubiszyn wynikające ze składu węglowodorów ciekłych w dolomicie głównym. *Przegląd Geologiczny* 46, 171-177.
- da Cruz, F.G., de Vasconcellos, S.P., Angolini, C.F.F., Dellagnezze, B.M., Garcia, I.N.S., de Oliveira, V.M., dos Santos Neto, E.V., Marsaioli, A.J., 2011. Could petroleum biodegradation be a joint achievement of aerobic and anaerobic microorganisms in deep sea reservoirs? *AMB Express* 1, 47.
- Defays, D., 1977. An efficient algorithm for a complete link method. *The Computer Journal* 20, 364-366.
- Doornenbal, H., Stevenson, A., 2010. Petroleum geological atlas of the Southern Permian Basin area. EAGE Publication BV, 352 p.
- Edgell, H.S., 1991. Proterozoic salt basins of the Persian Gulf area and their role in hydrocarbon generation. *Precambrian Research* 54, 1-14.
- Farrimond, P., Bevan, J.C., Bishop, A.N., 1999. Tricyclic terpane maturity parameters: response to heating by an igneous intrusion. *Organic Geochemistry* 30, 1011-1019.
- French, K.L., Rocher, D., Zumbege, J.E., Summons, R.E., 2015. Assessing the distribution of sedimentary C<sub>40</sub> carotenoids through time. *Geobiology* 13, 139-151.
- Frimmel, A., Oschmann, W., Schwark, L., 2004. Chemostratigraphy of the Posidonia Black Shale, SW Germany: I. Influence of sea-level variation on organic facies evolution. *Chemical Geology* 206, 199-230.
- Fu, J., Sheng, G., Peng, P., Brassell, S.C., Eglinton, G., Jigang, J., 1986. Peculiarities of salt lake sediments as potential source rocks in China. *Organic Geochemistry* 10, 119-126.



- Gąsiewicz, A., 2013. Climatic control on the Late Permian Main Dolomite (Ca<sub>2</sub>) deposition in northern margin of the Southern Permian Basin and implications to its internal cyclicity. Geological Society, London, Special Publications 376, 475-521.
- Gerling, P., Piske, J., Rasch, H.-J., Wehner, H., 1996a. Paläogeographie, Organofazies und Genese von Kohlenwasserstoffen im Staßfurt-Karbonat Ostdeutschlands. 2. Genese von Erdölen und Erdölbegleitgasen. Erdöl Erdgas Kohle 112, 152-156.
- Gerling, P., Piske, J., Rasch, H.-J., Wehner, H., 1996b. Paläogeographie, Organofazies und Genese von Kohlenwasserstoffen im Staßfurt-Karbonat Ostdeutschlands. 1. Sedimentationsverlauf und Muttergesteinsausbildung. Erdöl Erdgas Kohle 112, 13-18.
- Grantham, P.J., 1986. The occurrence of unusual C<sub>27</sub> and C<sub>29</sub> sterane predominances in two types of Oman crude oil. Organic Geochemistry 9, 1-10.
- Grantham, P.J., Wakefield, L.L., 1988. Variations in the sterane carbon number distributions of marine source rock derived crude oils through geological times. Organic Geochemistry 12, 61-77.
- Grelowski, C., Czechowski, F., 2011. Diversity of source, biomarkers composition and maturity of crude oils in Zechstein Main Dolomite deposits, NW Poland. 25<sup>th</sup> International Meeting on Organic Geochemistry, 18-23 September, Interlaken, Switzerland. Book of abstracts, p. 242.
- Grice, K., Schaeffer, P., Schwark, L., Maxwell, J.R., 1996. Molecular indicators of palaeoenvironmental conditions in an immature Permian shale (Kupferschiefer, Lower Rhine Basin, north-west Germany) from free and S-bound lipids. Organic Geochemistry 25, 131-147.
- Grice, K., Schouten, S., Nissenbaum, A., Charrach, J., Sinninghe Damsté, J.S., 1998. Isotopically heavy carbon in the C<sub>21</sub> to C<sub>25</sub> regular isoprenoids in halite-rich deposits from the Sdom Formation, Dead Sea Basin, Israel. Organic Geochemistry 28, 349-359.
- Hammes, U., Schulz, H.-M., Bechtel, A., 2014. Northern German unconventional reservoirs in Upper Permian (Ca<sub>2</sub>) microbial slope and basin dolomitized mudstones: assessment of oil to source-rock correlations within a sequence stratigraphic framework. Search and Discovery Article #80238.
- Hays, L.E., Grice, K., Foster, C.B., Summons, R.E., 2012. Biomarker and isotopic trends in a Permian-Triassic sedimentary section at Kap Stosch, Greenland. Organic Geochemistry 43, 67-82.
- Hiete, M., Berner, U., Heunisch, C., Röhling, H. 2005. A high resolution inorganic geochemical profile across the Zechstein-Buntsandstein boundary in the North German Basin. Zeitschrift der Deutschen Gesellschaft für Geowissenschaften 157, 77-106.

- Hindenberg, K., 1999. Genese, Migration und Akkumulation von Erdöl in Mutter- und Speichergesteinendes Staßfurt-Karbonat (Ca<sub>2</sub>) von Mecklenburg-Vorpommern und Südost-Brandenburg. Bericht des FZ Jülich, No 3698, 184 pp.
- Hofmann, P., Leythaeuser, D., 1995. Migration of hydrocarbons in carbonate source rocks of the Staßfurt member (Ca<sub>2</sub>) of the Permian Zechstein, borehole Aue 1, Germany: the role of solution seams. *Organic Geochemistry* 23, 597-606.
- Hounslow, M.W., Balabanov, Y.P., *in press*. A geomagnetic polarity timescale for the Permian, calibrated to stage boundaries. Geological Society, London, Special Publications 450, <https://doi.org/10.1144/SP450.8>
- Huang, W.-Y., Meinschein, W.G., 1979. Sterols as ecological indicators. *Geochimica et Cosmochimica Acta* 43, 739-745.
- Huang, D., Li, J., Zhang, D., 1990. Maturation sequence of continental crude oils in hydrocarbon basins in China and its significance. *Organic Geochemistry* 16, 521-529.
- Hughes, W.B., Holba, A.G., Dzou, L.I.P., 1995. The ratios of dibenzothiophene to phenanthrene and pristane to phytane as indicators of depositional environment and lithology of petroleum source rocks. *Geochimica et Cosmochimica Acta* 59, 3581-3598.
- Jiamo, F., Guoying, S., Pingan, P., Brassell, S.C., Eglinton, G., Jigang, J., 1986. Peculiarities of salt lake sediments as potential source rocks in China. *Organic Geochemistry* 10, 119-126.
- Joachimski, M., Ostertag-Henning, C., Pancost, R.D., Strauss, H., Freeman, K.H., Littke, R., Sinninghe Damsté, J., Racki, G., 2001. Water column anoxia, enhanced productivity and concomitant changes in  $\delta^{13}\text{C}$  and  $\delta^{34}\text{S}$  across the Frasnian-Famennian boundary (Kowala-Holy Cross Mountains/Poland). *Chemical Geology* 175, 109-131.
- Jurisch, A., Krooss, B.M., 2008. A pyrolytic study of the speciation and isotopic composition of nitrogen in carboniferous shales of the North German Basin. *Organic Geochemistry* 39, 924-928.
- Karnin, W.-D., Idiz, E., Merkel, D., Ruprecht, E., 1996. The Zechstein Stassfurt Carbonate hydrocarbon system of the Thuringian Basin, Germany. *Petroleum Geoscience* 2, 53-58.
- Katz, B.J., Elrod, L.W., 1983. Organic geochemistry of DSDP Site 467, offshore California, Middle Miocene to Lower Pliocene strata. *Geochimica et Cosmochimica Acta* 47, 389-396.
- Kenig, F., Hudson, J.D., Sinninghe Damsté, J.S., Popp, B.N., 2004. Intermittent euxinia: reconciliation of a Jurassic black shale with its biofacies. *Geology* 32, 421-424.

791 Kirkland, D.W., Evans, R., 1981. Source-rock potential of evaporitic environment. AAPG Bulletin 65,  
792 181-190.

793 Kodner, R.B., Pearson, A., Summons, R.E., Knoll, A.H., 2008. Sterols in red and green algae:  
794 quantification, phylogeny, and relevance for the interpretation of geologic steranes. Geobiology 6,  
795 411-420.

796 Koopmans, M.P., Köster, J., Van Kaam-Peters, H.M.E., Kenig, F., Schouten, S., Hartgers, W.A., de  
797 Leeuw, J.W., Sinninghe Damsté, J.S., 1996. Diagenetic and catagenetic products of isorenieratene:  
798 molecular indicators for photic zone anoxia. Geochimica et Cosmochimica Acta 60, 4467-4496.

799 Kosakowski, P., Krajewski, M., 2014. Hydrocarbon potential of the Zechstein Main Dolomite in the  
800 western part of the Wielkopolska platform, SW Poland: New sedimentological and geochemical data.  
801 Marine and Petroleum Geology 49, 99-120.

802 Kosakowski, P., Krajewski, M., 2015. Hydrocarbon potential of the Zechstein Main Dolomite (Upper  
803 Permian) in western Poland: Relation to organic matter and facies characteristics. Marine and  
804 Petroleum Geology 68, 675-694.

805 Kotarba, M.J., Koltun, Y.V., 2006. Origin and habitat of hydrocarbons of the Polish and Ukrainian  
806 parts of the Carpathian Province. AAPG Memoir 84, 395-443.

807 Kotarba, M., Wagner, R., 2007. Generation potential of the Zechstein Main Dolomite (Ca<sup>2</sup>)  
808 carbonates in the Gorzów Wielkopolski-Międzychód-Lubiatów area: geological and geochemical  
809 approach to microbial-algal source rock. Przegląd Geologiczny 55, 1025-1036.

810 Kotarba, M., Więclaw, D., Kowalski, A., 1998. Geneza gazu ziemnego i ropy naftowej z wybranych  
811 obszarów basenu dewońskiego i cechsztyńskiego Niżu Polskiego w świetle badań geochemicznych.  
812 Prace Państwowego Instytutu Geologicznego 165, 261-272.

813 Kotarba, M., Więclaw, D., Kowalski, A., 2000. Skład, geneza i środowisko generowania ropy  
814 naftowej w utworach dolomitu głównego zachodniej części obszaru przedsudeckiego. Przegląd  
815 Geologiczny 48, 436-442.

816 Kotarba, M., Kosakowski, P., Więclaw, D., Kowalski, A., 2003. Potencjał naftowy utworów dolomitu  
817 głównego w strefie Kamienia Pomorskiego. Część 1 – Macierzystość. Przegląd Geologiczny 51, 587-  
818 594.

819 Kotarba, M.J., Więclaw, D., Koltun, Y.V., Marynowski, L., Kuśmerek, J., Dudok, I.V., 2007.  
820 Organic geochemical study and genetic correlation of natural gas, oil and Menilite source rocks in the

area between San and Stryi rivers (Polish and Ukrainian Carpathians). *Organic Geochemistry* 38, 1431–1456.

Kotarba, M.J., Bilkiewicz, E., Hałas, S., 2017. Mechanisms of generation of hydrogen sulphide, carbon dioxide and hydrocarbon gases from selected petroleum fields of the Zechstein Main Dolomite carbonates of the western part of Polish Southern Permian Basin: Isotopic and geological approach. *Journal of Petroleum Science and Engineering* 157, 380-391.

Krooss, B.M., Littke, R., Müller, B., Frielingsdorf, J., Schwochau, K., Idiz, E.F., 1995. Generation of nitrogen and methane from sedimentary organic matter: Implications on the dynamics of natural gas accumulations. *Chemical Geology* 126, 291-318.

Krooss, B.M., Friberg, L., Gensterblum, Y., Hollenstein, J., Prinz, D., Littke, R., 2005. Investigation of the pyrolytic molecular nitrogen from Palaeozoic sedimentary rocks. *International Journal of Earth Sciences* 94, 1023-1038.

Krooss, B.M., Jurisch, A., Plessen, B., 2006. Investigation of the fate of nitrogen in Palaeozoic shales of the Central European Basin. *Journal of Geochemical Exploration* 89, 191-194.

Lott, G., Wong, T., Dusa, M., Andsbjerg, J., Mönning, E., Feldman-Olszewska, A., Verreussel, R., 2010. Jurassic. In: Doornenbal, J.C., Stevenson, A.G. (ed.), *Petroleum geological atlas of the Southern Permian Basin area* Eage Publications b.v. (Houten), p. 175-193.

Mello, M.R., Telnaes, N., Gaglianone, P.C., Chicarelli, M.I., Brassell, S.C., Maxwell, J.R., 1988a. Organic geochemical characterisation of depositional palaeoenvironments of source rocks and oils in Brazilian marginal basins. *Organic Geochemistry* 13, 31-45.

Mello, M.R., Gaglianone, P.C., Brassell, S.C., Maxwell, J.R., 1988b. Geochemical and biological marker assessment of depositional environments using Brazilian offshore oils. *Marine and Petroleum Geology* 5, 205–223.

Mello, M.R., Koutsoukos, E.A.M., Hart, M.B., Brassell, S.C., Maxwell, J.R., 1990. Late Cretaceous anoxic events in the Brazilian continental margin. *Organic Geochemistry* 14, 529–542.

Mikołajewski, Z., Czechowski, F., Grelowski, C., 2012. Charakterystyka geologiczno-litofacjalno-geochemiczna złóż ropy naftowej w utworach dolomitu głównego w rejonie platformy węglanowej Kamienia Pomorskiego. *Prace Naukowe Instytutu Nafty i Gazu* 182, 387–397.

Mingram, B., Hoth, P., Lüders, V., Harlov, D., 2005. The significance of fixed ammonium in Palaeozoic sediments for the generation of nitrogen-rich natural gases in the North German Basin. *International Journal of Earth Sciences* 94, 1010-1022.

- Moldowan, J.M., Seifert, W.K., Gallegos, E.J., 1985. Relationship between petroleum composition and depositional environment of petroleum source rocks. *AAPG Bulletin* 69, 1255-68.
- Moldowan, J.M., Peters, K.E., Carlson, R.M.K., Schoell, M., Abu-Ali, M.A., 1994. Diverse applications of petroleum biomarker maturity parameters. *Arabian Journal for Science and Engineering* 19, 273-298.
- Moldowan, J.M., Lee, C.Y., Watt, D.S., Jeganathan, A., Slougui, N.-E., Gallegos, E.J., 1991. Analysis and occurrence of C<sub>26</sub>-steranes in petroleum and source rocks. *Geochimica et Cosmochimica Acta* 55, 1065-1081.
- Müller, E.P., 1984. Zur Genese von Erdölen in Karbonaten am Beispiel der Lagerstätten des Oberen Perm des Territoriums der DDR. *Zeitschrift für angewandte Geologie* 30, 214-218.
- Palacas, J.G., 1984. Carbonate rocks as sources of petroleum: geological and chemical characteristics and oil-source correlations. *Proceedings of the 11<sup>th</sup> World Petroleum Congress 1983*, Vol. 2, John Wiley & Sons, Chichester, UK, pp. 31-43.
- Palacas, J.G., Anders, D.E., King, J.D., 1984. South Florida Basin – a prime example of carbonate source rocks of petroleum. *AAPG Studies in Geology* 18, 71-96.
- Paul, J., 2010. Zur Zyklizität und Dauer des Zechsteins. *Zeitschrift der Deutschen Gesellschaft für Geowissenschaften* 161, 455-457.
- Peryt, T.M., Geluk, M., Mathiesen, A., Paul, J., Smith, K., 2010. Zechstein. In: Doornenbal, J.C., Stevenson, A.G. (eds), *Petroleum Geological Atlas of the Southern Permian Basin Area*. EAGE Publications b.v. (Houten), p. 123-147.
- Peters, K.E., Moldowan, J.M., 1991. Effects of source, thermal maturity, and biodegradation on the distribution and isomerization of homohopanes in petroleum. *Organic Geochemistry* 17, 47-61.
- Peters, K.E., Walters, C.C., Moldowan, J.M., 2005. *The Biomarker Guide*. Cambridge University Press, Cambridge, 1155 pp.
- Petersen, H.I., Hertle, M., Juhasz, A., Krabbe, H., 2016. Oil family typing, biodegradation and source rock affinity of liquid petroleum in the Danish North Sea. *Journal of Petroleum Geology* 39, 247-268.
- Pharaoh, T.C., Dusa, M., Geluk, M.C., Kockel, F., Krawczyk, C.M., Krzywiec, P., Schenk-Wenderoth, M., Thybo, H., Vejbaek, van Wees, J.D., 2010. Tectonic evolution. In: Doornenbal, J.C., Stevenson, A.G. (eds), *Petroleum Geological Atlas of the Southern Permian Basin Area*. Eage Publications b.v. (Houten), p. 25-57.

883 Philp, R.P., Chen, J.H., Fu, J.M., Sheng, G.Y., 1992. A geochemical investigation of crude oils and  
884 source rocks from Biyang Basin, China. *Organic Geochemistry* 18, 933-945.

885 Pletsch, T., Appel, J., Botor, D., Clayton, C., Duin, E., Faber, E., Górecki, W., Kombrink, H.,  
886 Kosakowski, P., Kuper, G., Kus, J., Lutz, R., Mathiesen, A., Ostertag-Henning, C., Papiernik, B., van  
887 Bergen, F., 2010. Petroleum generation and migration. In: Doornenbal, J.C., Stevenson, A.G. (eds),  
888 Petroleum Geological Atlas of the Southern Permian Basin Area. Eage Publications b.v. (Houten), p.  
889 225-253.

890 Radke, M., 1988. Application of aromatic compounds as maturity indicators in source rocks and crude  
891 oils. *Marine and Petroleum Geology* 5, 224-236.

892 Requejo, A.G., 1994. Maturation of petroleum source rocks—II. Quantitative changes in extractable  
893 hydrocarbon content and composition associated with hydrocarbon generation. *Organic Geochemistry*  
894 21: 91-105.

895 Richter-Bernburg, G., 1953. Stratigraphische Gliederung des deutschen Zechsteins. *Zeitschrift der*  
896 *Deutschen Geologischen Gesellschaft* 105, 843-854.

897 Schoell, M., 1984. Wasserstoff- und Kohlenstoffisotope in organischen Substanzen, Erdölen und  
898 Erdgasen. *Geologische Jahrbuch D67*, 167pp.

899 Schwark, L., Vliex, M., Karnin, W.-D., Waldmann, R., 1998. Geochemische Untersuchungen an  
900 ausgewählten Mutter- und Speichergesteinen des Zechsteins am Beispiel der Bohrung Sprötau Z1  
901 (Thüringen Becken). *Geologische Jahrbuch A149*, 185-211.

902 Seifert, W.K., Moldowan, J.M., 1978. Applications of steranes, terpanes and monoaromatics to the  
903 maturation, migration and source of crude oils. *Geochimica et Cosmochimica Acta* 42, 77-95.

904 Seifert, W.K., Moldowan, J.M., 1979. The effect of biodegradation on steranes and terpanes in crude  
905 oils. *Geochimica et Cosmochimica Acta* 43, 111-126.

906 Seifert, W.K., Moldowan, J.M., 1986. Use of biological markers in petroleum exploration. *Methods in*  
907 *Geochemistry and Geophysics* 24, 261-290.

908 Shanmugam, G., 1985. Significance of coniferous rain forest and related organic matter in generating  
909 commercial quantities of oils, Gippsland Basin, Australia. *AAPG Bulletin* 69, 1241-1254.

910 Simoneit, B.R., Schoell, M., Dias, R.F., de Aquino Neto, F.R., 1993. Unusual carbon isotope  
911 compositions of biomarker hydrocarbons in a Permian tasmanite. *Geochimica et Cosmochimica Acta*  
912 57, 4205-4211.

913 Sinninghe Damsté, J.S., Wakeham, S.G., Kohnen, M.E.L., Hayes, J.M., de Leeuw, J.W., 1993. A  
914 6,000-year sedimentary molecular record of chemocline excursions in the Black Sea. *Nature* 362,  
915 827-829.

916 Sinninghe Damsté, J.S., Van Duin, A.C.T., Hollander, D., Kohnen, M.E.L., de Leeuw, J.W., 1995a.  
917 Early diagenesis of bacteriohopanepolyol derivatives: formation of fossil homohopanoids.  
918 *Geochimica et Cosmochimica Acta* 59, 5141-5155.

919 Sinninghe Damsté, J.S., Kenig, F., Koopmans, M.P., Köster, J., Schouten, S., Hayes, J.M., de Leeuw,  
920 J.W., 1995b. Evidence for gammacerane as an indicator of water column stratification. *Geochimica et*  
921 *Cosmochimica Acta* 59, 1895-1900.

922 Słowakiewicz, M., Mikołajewski, Z., 2009. Sequence stratigraphy of the Upper Permian Zechstein  
923 Main Dolomite carbonates in western Poland: a new approach. *Journal of Petroleum Geology* 32,  
924 215-234.

925 Słowakiewicz, M., Mikołajewski, Z., Sikorska, M., Poprawa, P., 2010. Origin of diagenetic fluids in  
926 the Zechstein Main Dolomite reservoir rocks, West Pomerania, Poland. *Zeitschrift der Deutschen*  
927 *Gesellschaft für Geowissenschaften* 161, 25-38.

928 Słowakiewicz, M., Mikołajewski, Z., 2011. Upper Permian Main Dolomite microbial carbonates as  
929 potential source rocks for hydrocarbons (W Poland). *Marine and Petroleum Geology* 28, 1572-1591.

930 Słowakiewicz, M., Gąsiewicz, A., 2013. Palaeoclimatic imprint, distribution and genesis of Zechstein  
931 Main Dolomite (Upper Permian) petroleum source rocks in Poland: Sedimentological and  
932 geochemical rationales. *Geological Society, London, Special Publications* 376, 523-538.

933 Słowakiewicz, M., Tucker, M.E., Pancost, R.D., Perri, E., Mawson, M., 2013. Upper Permian  
934 (Zechstein) microbialites: Supratidal through deep subtidal deposition, source rock, and reservoir  
935 potential. *AAPG Bulletin* 97, 1921-1936.

936 Słowakiewicz, M., Tucker, M.E., Perri, E., Pancost, R.D., 2015. Nearshore euxinia in the photic zone  
937 of an ancient sea. *Palaeogeography, Palaeoclimatology, Palaeoecology* 426, 242-259.

938 Słowakiewicz, M., 2016. Characteristic biomarkers in organic matter from three Zechstein (Late  
939 Permian) carbonate units. *Zeitschrift der Deutschen Gesellschaft für Geowissenschaften* 167, 269-279.

940 Słowakiewicz, M., Tucker, M.E., Hindenberg, K., Mawson, M., Idiz, E.F., Pancost, R.D., 2016a.  
941 Nearshore euxinia in the photic zone of an ancient sea: Part II – The bigger picture and implications  
942 for understanding ocean anoxia. *Palaeogeography, Palaeoclimatology, Palaeoecology* 461, 432-448.

943 Słowakiewicz, M., Perri, E., Tucker, M.E., 2016b. Micro- and nanopores in tight Zechstein 2  
 944 Carbonate facies from the Southern Permian Basin, NW Europe. *Journal of Petroleum Geology* 39,  
 945 149-168.

946 Sofer, Z., 1984. Stable carbon isotope compositions of crude oils: application to source depositional  
 947 environments and petroleum alteration. *AAPG Bulletin* 68, 31-49.

948 Sonnenfeld, P., 1985. Evaporites as oil and gas source rocks. *Journal of Petroleum Geology* 8, 253-  
 949 271.

950 Summons, R.E., Powell, T., 1986. Chlorobiaceae in Palaeozoic seas revealed by biological markers,  
 951 isotopes and geology. *Nature* 319, 763-765.

952 Szurlies, M., 2013. Late Permian (Zechstein) magnetostratigraphy in Western and Central Europe.  
 953 Geological Society, London, Special Publications 376, 73-85.

954 Taylor, J.C.M., 1998. Upper Permian – Zechstein. In: Glennie, K.W. (ed.), *Petroleum geology of the*  
 955 *North Sea*. Blackwell Science, 4<sup>th</sup> edition, 174-212.

956 Ten Haven, H.L., de Leeuw, J.W., Sinninghe Damsté, J.S., Schenck, P.A., Palmer, S.E., Zumberge,  
 957 J.E., 1988. Application of biological markers in the recognition of palaeohypersaline environments.  
 958 In: Fleet, A.J., Kelts, K., and Talbot, M.R. (ed.), *Lacustrine petroleum source rocks*. Geological  
 959 Society London, Special Publications 40, 123-130.

960 van Kaam-Peters, H.M.E., Rijpstra, W.I.C., de Leeuw, J.W., Sinninghe Damsté, J.S., 1998. A high  
 961 resolution biomarkers study of different lithofacies or organic sulfur-rich carbonate rocks of a  
 962 Kimmeridgian lagoon (French southern Jura). *Organic Geochemistry* 28, 151-177.

963 Volkman, J., 1986. A review of sterol markers for marine and terrigenous organic matter. *Organic*  
 964 *Geochemistry* 9, 83-99.

965 Volkman, J., Barrett, S., Blackburn, S., Mansour, M., Sikes, E., Gelin, F., 1998. Microalgal  
 966 biomarkers: a review of recent research development. *Organic Geochemistry* 29, 1163-1180.

967 Van Graas, G.W., 1990. Biomarker maturity parameters for high maturities: Calibration of the  
 968 working range up to the oil/condensate threshold. *Organic Geochemistry* 16, 1025-1032.

969 Van Wees, J.-D., Stevenson, R.A., Ziegler, P.A., McCann, T., Dadlez, R., Gaupp, R., Narkiewicz, M.,  
 970 Bitzer, F., Scheck, M., 2000. On the origin of the Southern Permian Basin, Central Europe. *Marine*  
 971 *and Petroleum Geology* 17, 43-49.



Wagner, R., 2012. Mapa paleogeograficzna dolomitu głównego (Ca<sub>2</sub>) w Polsce. Państwowy Instytut Geologiczny, unpublished.

Walters, C.C., Cassa, M.R., 1985. Regional organic geochemistry of offshore Louisiana. Gulf Coast Association of Geological Societies Transactions 35, 277-286.

Waples, D.W., Machihara, R., 1991. Biomarkers for geologists: a practical guide to the application of steranes and triterpanes in petroleum geology. AAPG Methods in Exploration Series 9, 91 pp.

Warren, J.K., 1986. Shallow water evaporitic environments and their source rock potential. Journal of Sedimentary Petrology 56, 442-454.

Warren, J.K., 2011. Evaporitic source rocks: mesohaline responses to cycles of 'famine or feast' in layered brines. IAS Special Publications 43, 315-392.

Wehner, H., 1997. Source and maturation of crude oils in northern and eastern Germany – an organic geochemical approach. Geologisches Jahrbuch D103, 85-102.

Zdanowski, P., Wozniak, K., 2010. Nitrogen source for the Main Dolomite natural gas in the Sulecin isolated platform area – verification of existing theory. 72<sup>nd</sup> EAGE Conference and Exhibition incorporating SPE EUROPEC 2010, J037.

Zhusheng, J., Philp, R.P., Lewis, C.A., 1988. Fractionation of biological markers in crude oils during migration and the effects on correlation and maturation parameters. Organic Geochemistry 13, 561-571.

Zumberge, J.E., Russell, J.A., Reid, S.A., 2005. Charging of Elk Hills reservoirs as determined by oil geochemistry. AAPG Bulletin 89, 1347-1371.

Captions to figures:

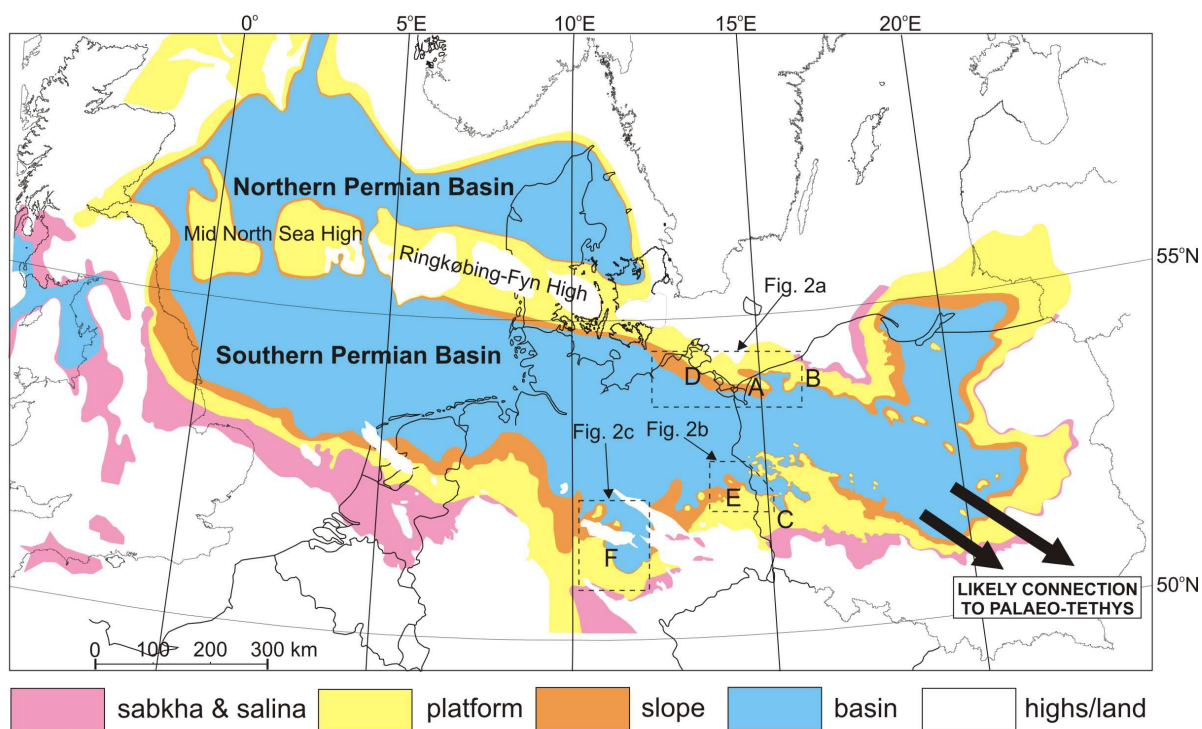
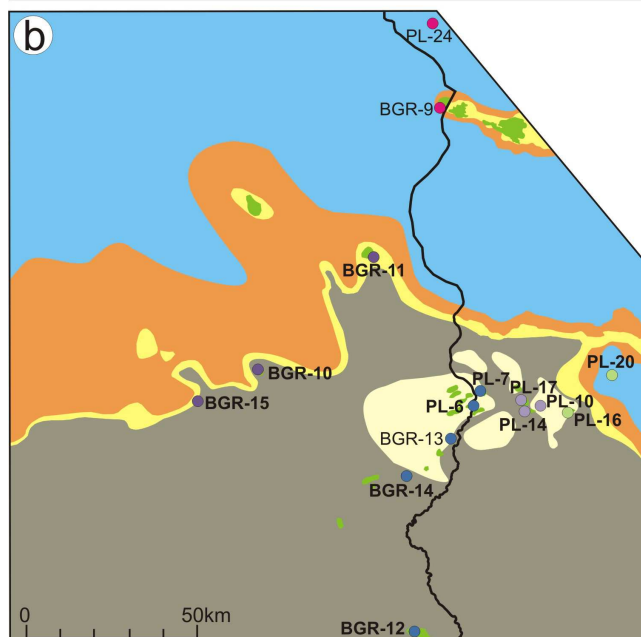
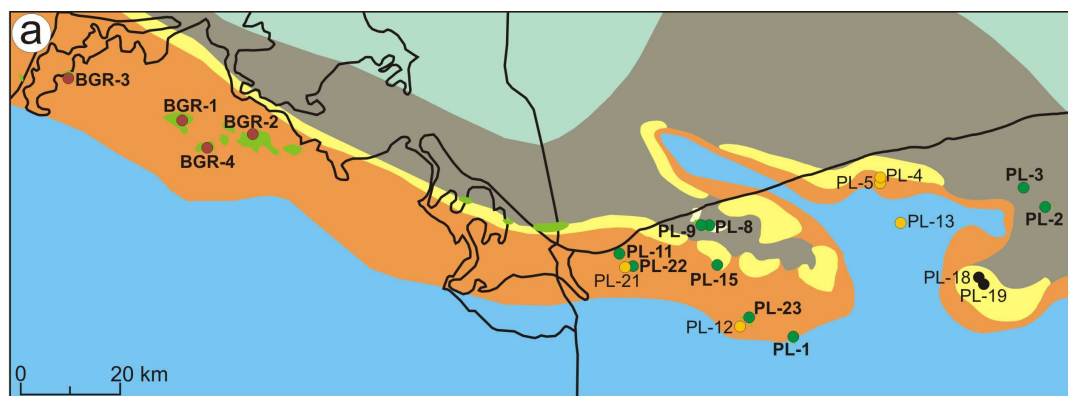


Fig. 1. Palaeoenvironmental map of the Ca2 in the Late Permian in Europe (updated after Słowakiewicz et al., 2015). Longitude and latitude are present day values. A – Kamień Pomorski carbonate platform; B – Pomerania carbonate platform; C – Fore-Sudetic Monocline; D – NE North German (sub)-Basin (Mecklenburg-Vorpommern); E – SE North German (sub)-Basin (Brandenburg); F – Thuringian (sub)-Basin.



SYSTEM		LITHOSTRATIGRAPHY	
LATE PERMIAN	ZECHSTEIN	Z3	Y. Halite + Y. Potash
			Main Anhydrite (A3)
			Platy Dolomite (Ca3)
			Grey Pelite (T3)
		Z2	Screening Anhydrite (A2r)
			Screening Older Halite (Na2r)
			Older Potash (K2)
			Older Halite (Na2)
		Z1	Basal Anhydrite (A2)
			Main Dolomite (Ca2)
			Upper Anhydrite (A1b)
			Oldest Halite (Na1)
Lower Anhydrite (A1a)			
Zechstein Limestone (Ca1)			
	Kupferschiefer (T1)		
UPPER ROTLIEGEND			

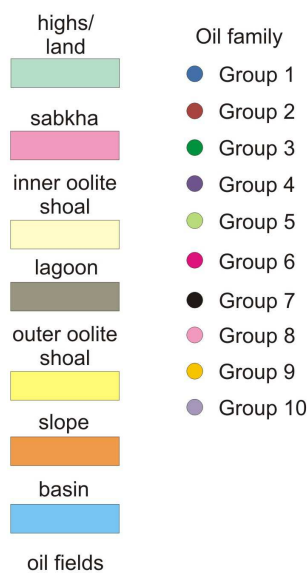


Fig. 2. Palaeoenvironmental maps, lithostratigraphy, and location of Ca2 oils in a) NW Poland and NE Germany; b) SW Poland and SE Germany; and c) Thuringian sub-basin, central-south Germany (modified after Hindenberg, 1999; Słowakiewicz et al., 2010; Brosin, 2013; Wagner, 2012; Gąsiewicz, 2013). Y. Halite + Y. Potash – Younger Halite (Na3) + Younger Potash (K3); Z1, Z2, Z3 – Zechstein cycles 1, 2, 3. Well names in bold font indicate crude oils containing isorenieratane.

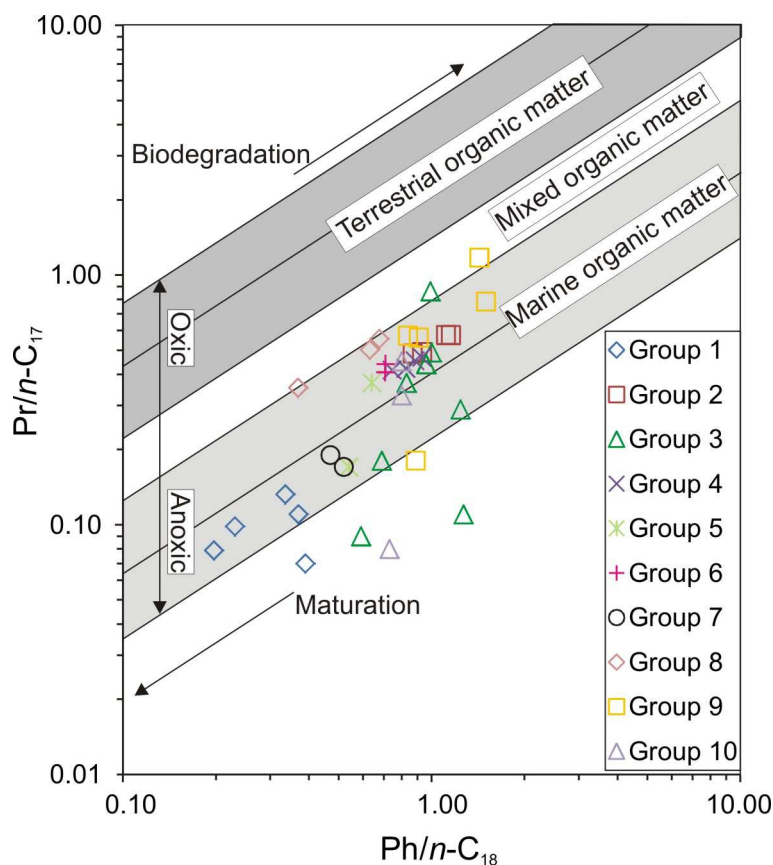


Fig. 3. Phytane to  $n$ -C<sub>18</sub> alkane (Ph/ $n$ -C<sub>18</sub>) versus pristane to  $n$ -C<sub>17</sub> alkane (Pr/ $n$ -C<sub>17</sub>) for Ca2 oil samples (graphical fields are according to Shanmugam, 1985).

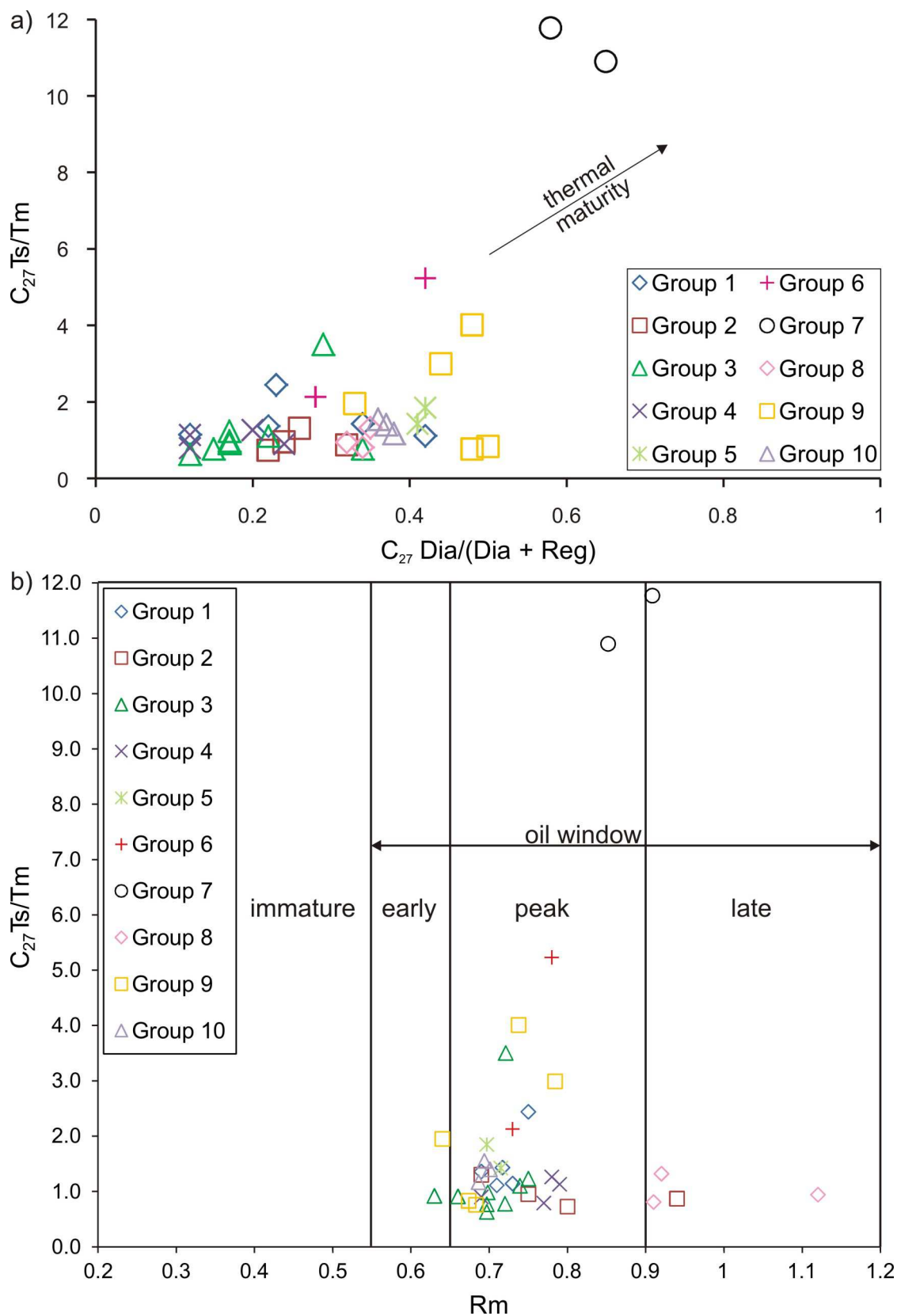


Fig. 4.  $C_{27}$  18 $\alpha$ -trisnorneohopane/17 $\alpha$ -trisnorhopane (Ts/Tm) versus other geochemical ratios indicating thermal maturity of Ca2 oils. a) Ts/Tm versus  $C_{27}$  diasteranes/(diasteranes + regular steranes) [ $C_{27}$  Dia/(Dia + Reg)] shows thermal maturity control of Ca2 oil samples; b) Ts/Tm versus calculated vitrinite reflectance ( $R_m$ ; Radke, 1988) grouping the majority of Ca2 oil samples within the peak oil window.

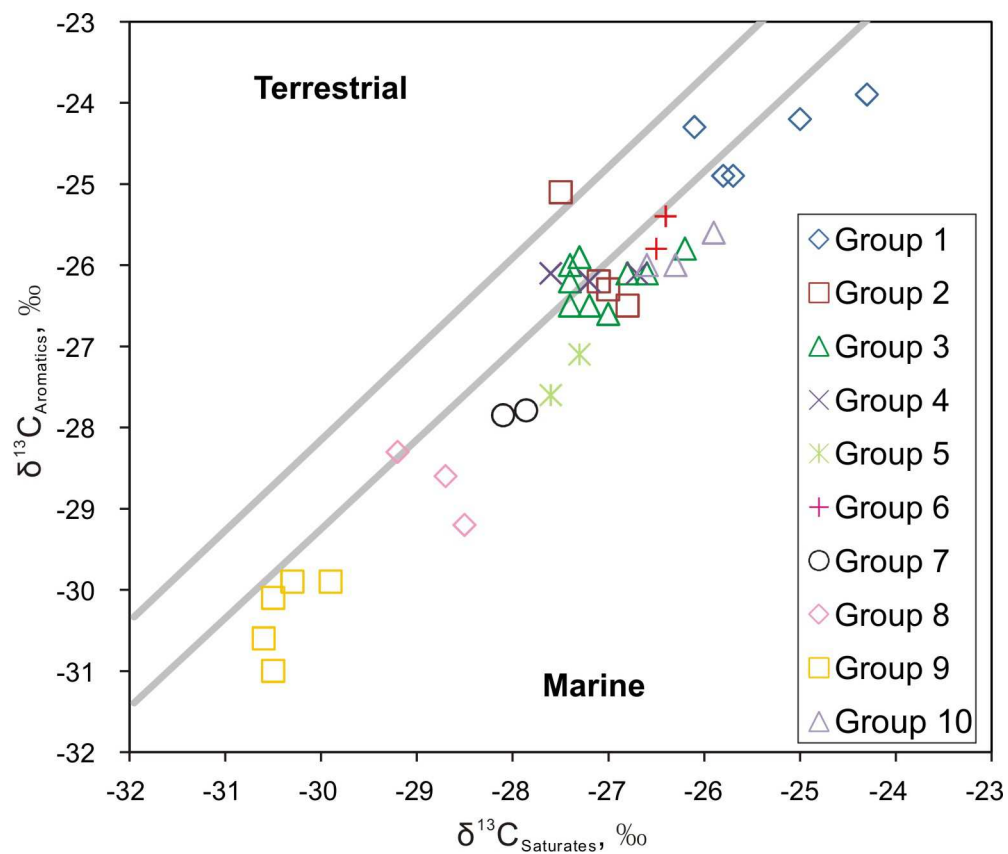
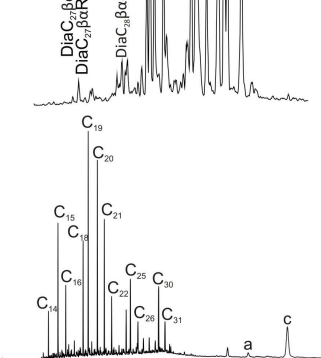
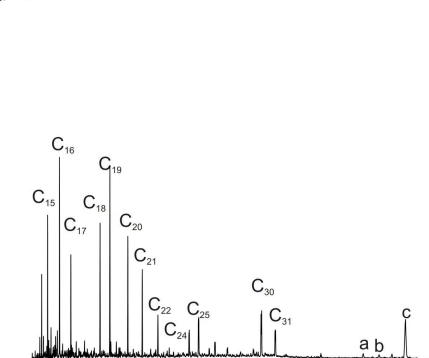
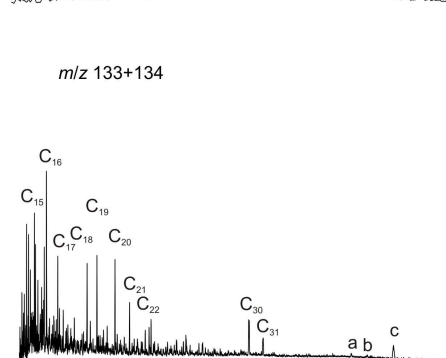
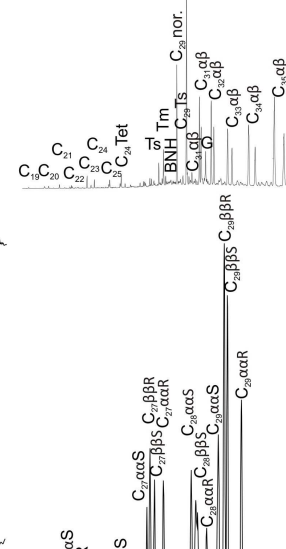
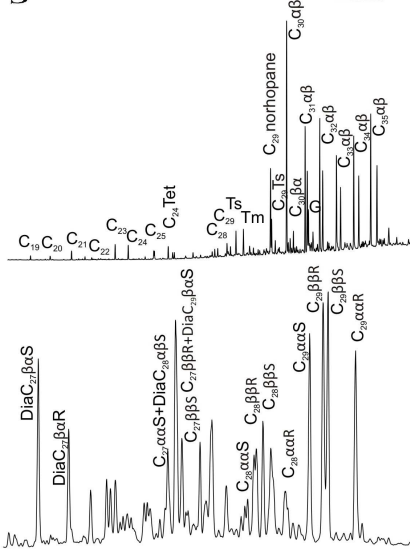
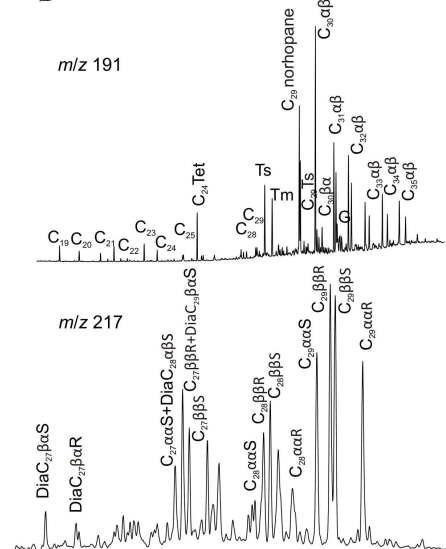
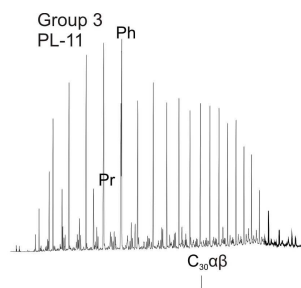
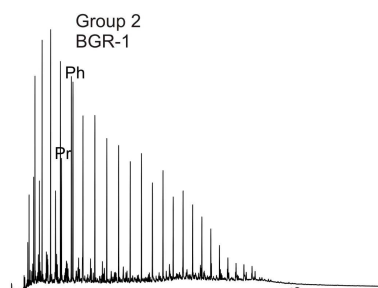
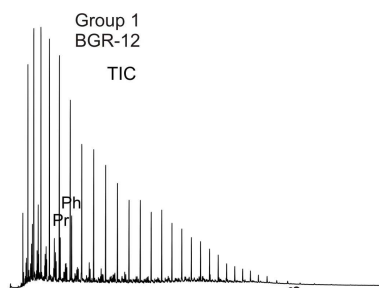
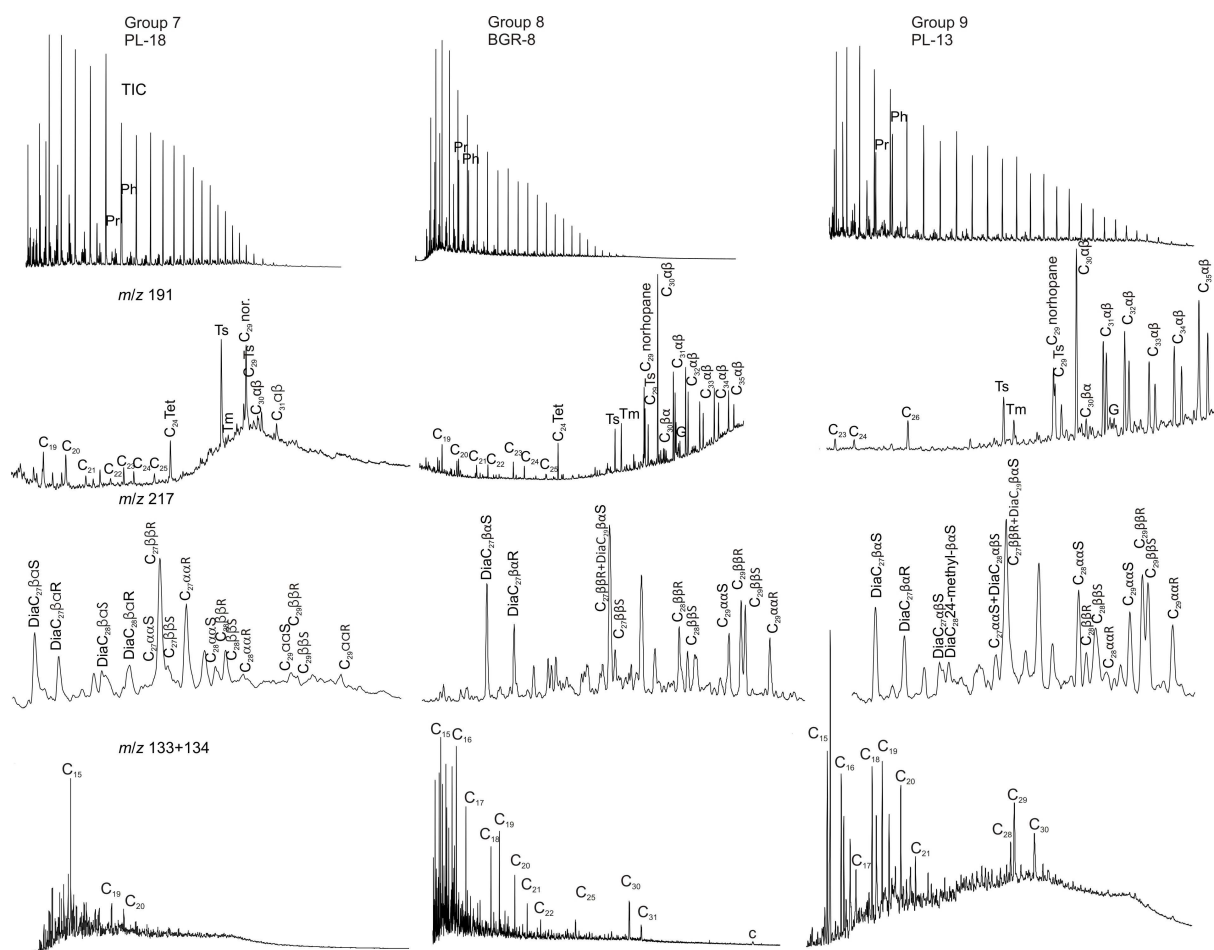


Fig. 5. Sofer's (1984) plot of  $\delta^{13}\text{C}$  values for the saturated and aromatic fractions for Ca2 oils located in Germany and Poland.









Group 10  
PL-10

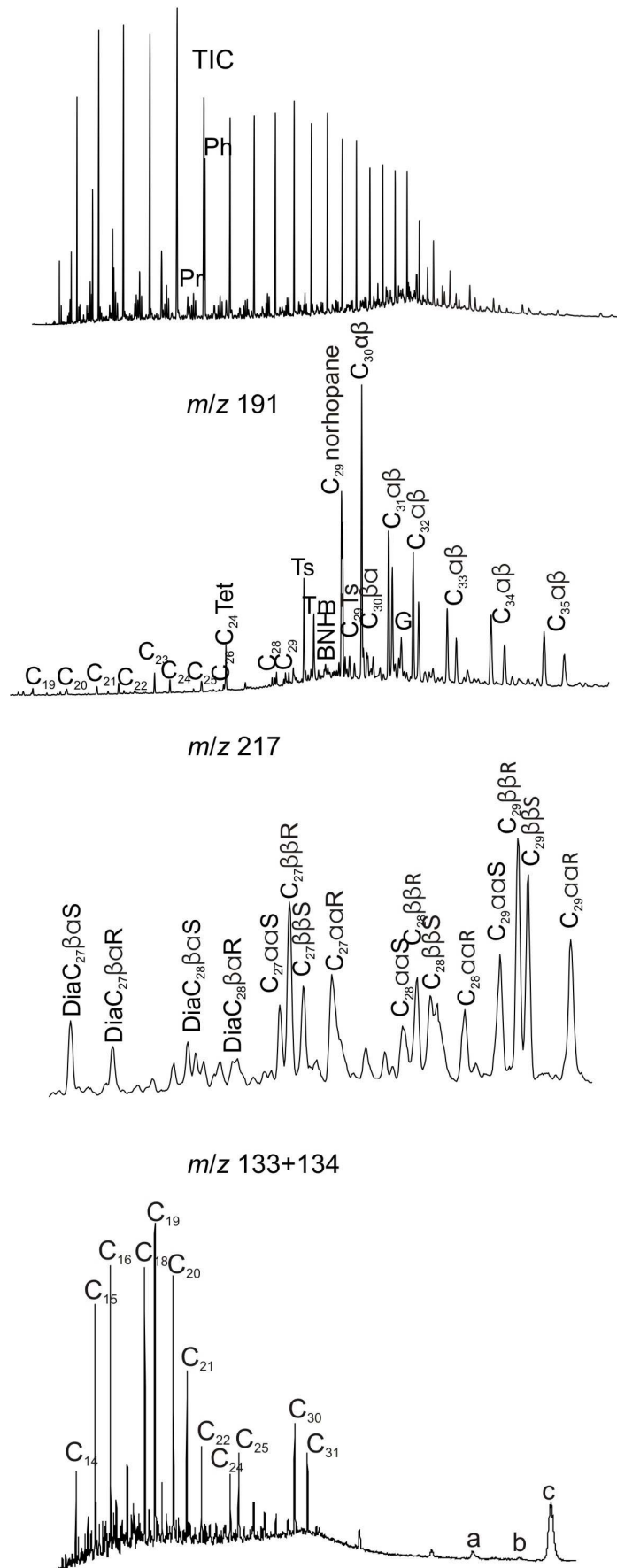
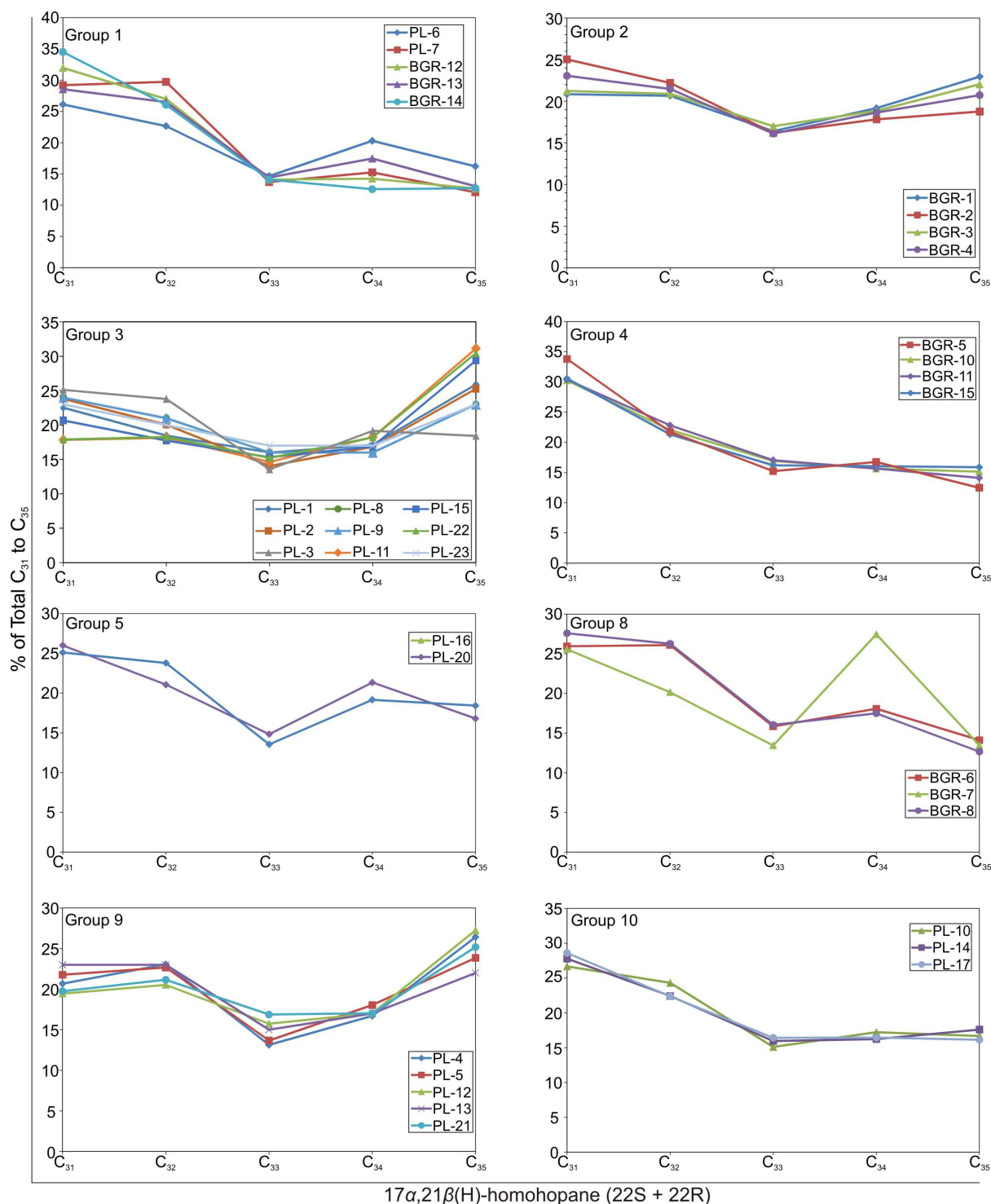
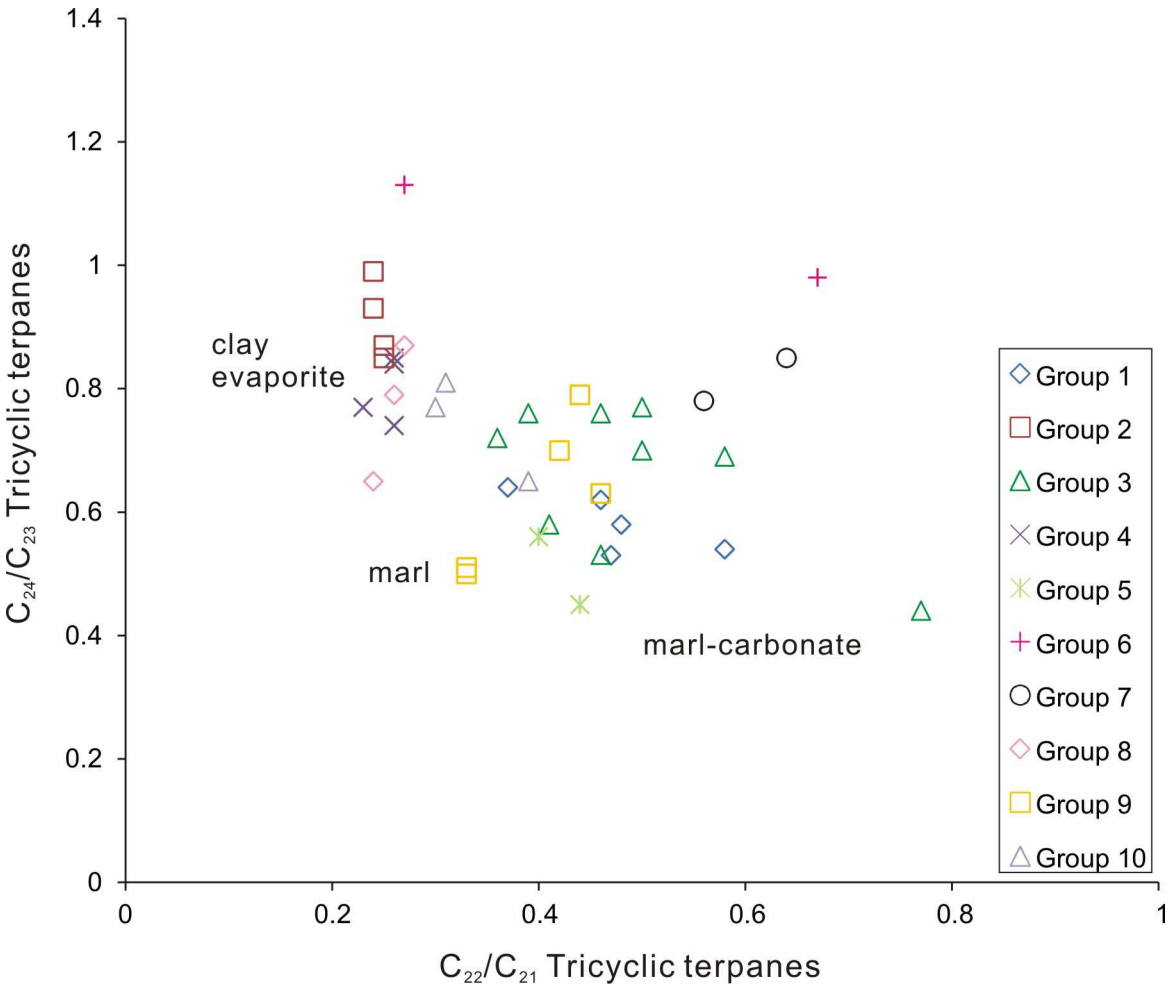


Fig. 6. Representative total ion current chromatograms of whole oils (TIC) and mass chromatograms ( $m/z$  191,  $m/z$  217,  $m/z$  133+134) of the saturated and aromatic fractions of Ca2 oils showing the correlation of ten oil groups. Ts –  $C_{27}$  18 $\alpha$ -trisorneohopane; Tm - 17 $\alpha$ -trisnorhopane; a – chlorobactane; b –  $\beta$ -isorenieratane; c – isorenieratane. Other symbols as in Table 1. Note that tricyclic terpanes in groups 6 and 7 have quite low abundance with respect to the overall high thermal maturity of the oil samples, which could result from the lithological type of the source rocks or alteration effects.



1027 Fig. 7. Homohopane distributions in Ca2 oils. BGR-9, PL-18, -19 and -24 are not plotted because of absent or  
 1028 reduced homohopanes.



1029  
 1030 Fig. 8. C<sub>24</sub>/C<sub>23</sub> versus C<sub>22</sub>/C<sub>21</sub> of tricyclic terpanes for the studied oils used to infer source rock lithology from oil  
 1031 composition (Peters et al., 2005).  
 1032

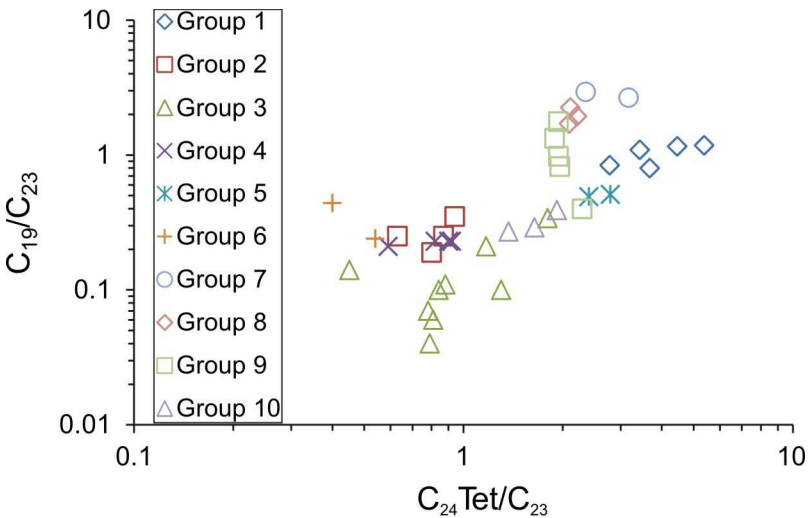


Fig. 9.  $C_{24}$  tetracyclic (Tet)/ $C_{23}$  tricyclic terpanes versus  $C_{19}/C_{21}$  tricyclic terpanes for Ca2 oil samples used to infer source rock lithology from oil composition. Oil groups are differentiated and facies-controlled. High abundance of  $C_{24}$  Tet might indicate carbonate-evaporite depositional environment of source rocks for Ca2 oils.

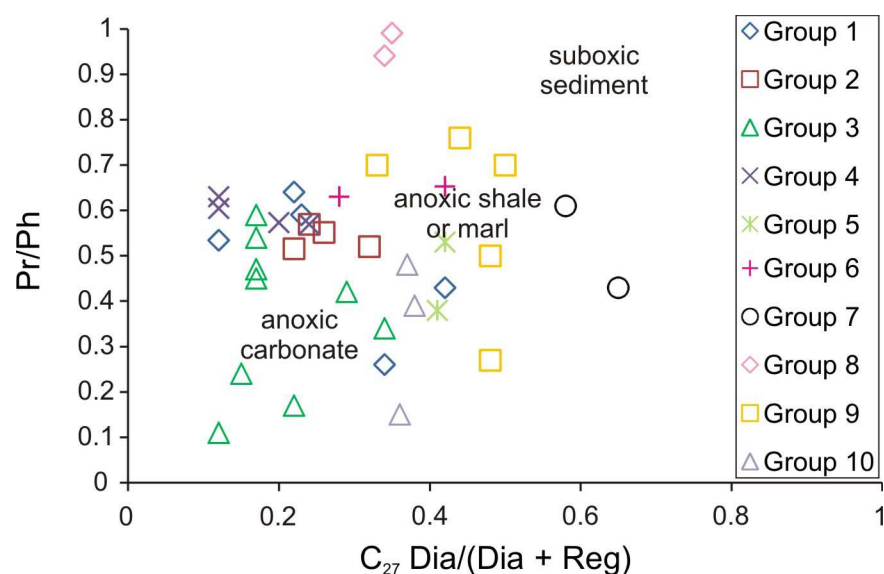


Fig. 10. Correlation between pristane/phytane (Pr/Ph) and  $C_{27}$  diasteranes/(diasteranes + regular steranes) obtained from extracts of Ca2 oils showing that the correlation is controlled by the depositional environment of source rocks for Ca2 hydrocarbons (fields modified after Moldowan et al., 1994).

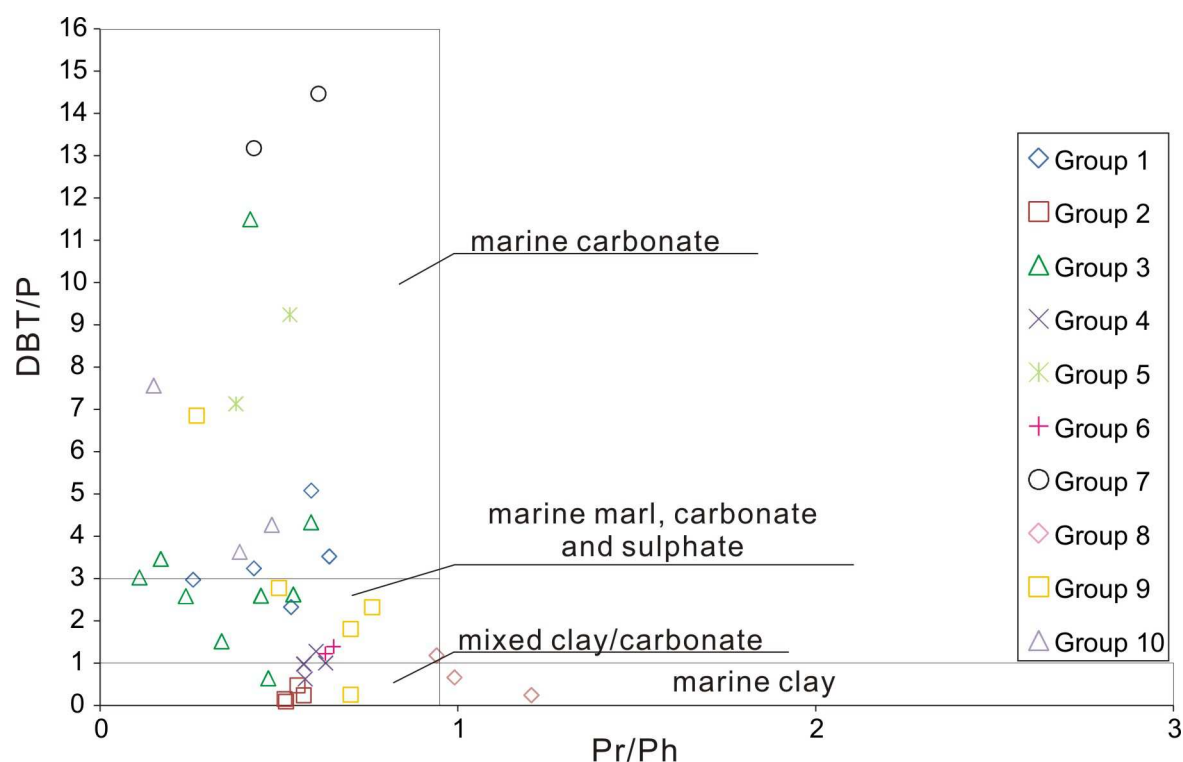


Fig. 11. Cross-plot of dibenzothiophene/phenanthrene (DBT/P) ratio versus pristane/phytane (Pr/Ph) ratio for Ca2 oil samples (graphical fields modified after Hughes et al., 1985).

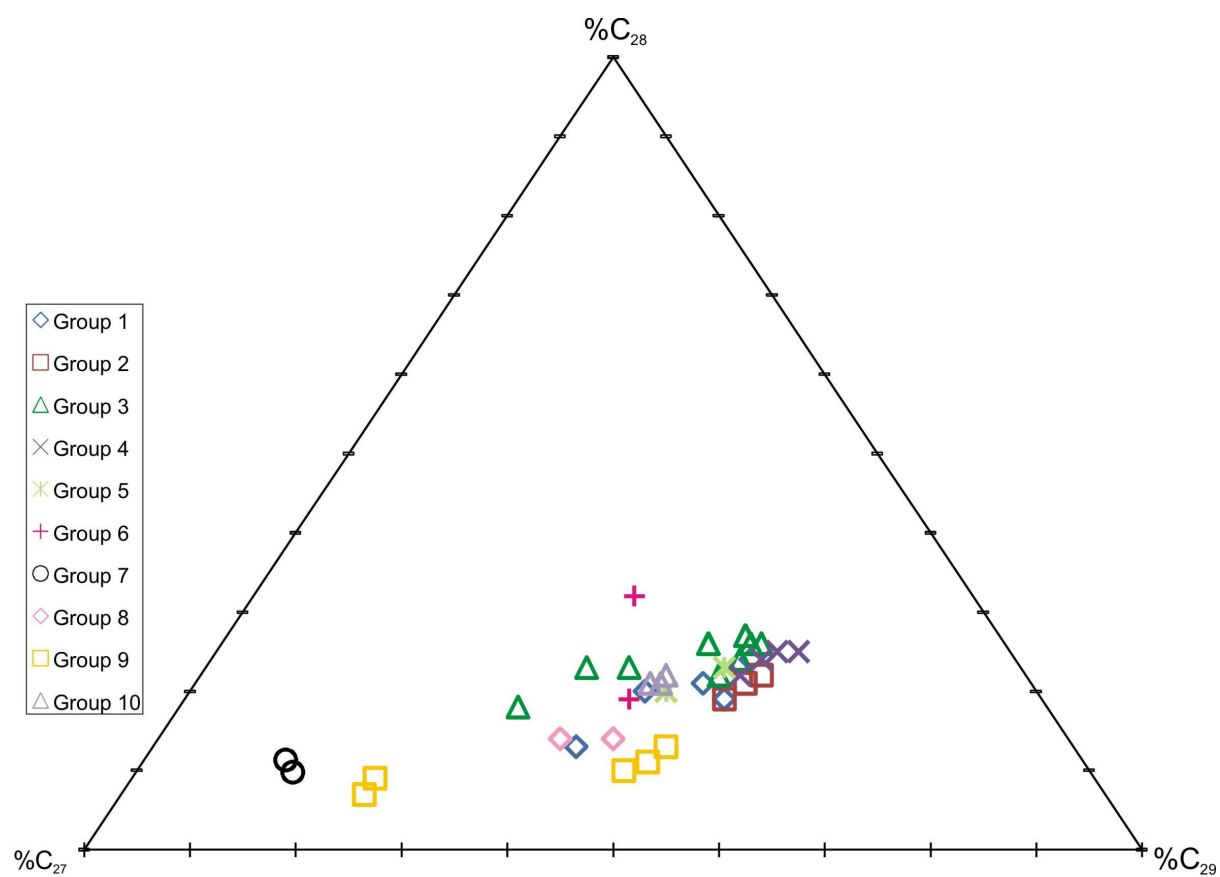


Fig. 12. Ternary diagram of  $C_{27}$ -,  $C_{28}$ -, and  $C_{29\alpha\alpha\alpha}$  (20R)-sterane distributions for the analysed Ca2 oil samples.

Group	Wells	Oil field	Depth (m)	$\delta^{13}\text{C}_{\text{SAT}}$	$\delta^{13}\text{C}_{\text{ARO}}$	CV	Pr/Ph	Pr/n - C <sub>17</sub>	Ph/n - C <sub>18</sub>	C <sub>19</sub> /C <sub>23</sub>	C <sub>22</sub> /C <sub>21</sub>	C <sub>24</sub> /C <sub>23</sub>	C <sub>24</sub> Tet/C <sub>23</sub>	C <sub>26</sub> /C <sub>25</sub>
1	BGR-12	Döbern	-	-25.8	-24.9	-1.65	0.53	0.13	0.34	0.84	0.37	0.64	2.78	1.01
1	BGR-13	Guben	-	-25	-24.2	-2.12	0.64	0.08	0.20	1.16	0.58	0.54	4.45	0.92
1	BGR-14	Tauer	-	-26.1	-24.3	0.44	0.59	0.10	0.23	1.09	0.47	0.53	3.43	1
1	PL-6	Kosarzyn	1753.5-1788	-24.3	-23.9	-3.23	0.26	0.07	0.39	0.8	0.48	0.58	3.67	0.89
1	PL-7	Kosarzyn	1810.7-1817.5	-25.7	-24.9	-1.91	0.43	0.11	0.37	1.18	0.46	0.62	5.37	0.81
2	BGR-1	Richtenberg	-	-27	-26.3	-1.73	0.52	0.57	1.11	0.25	0.24	0.93	0.87	0.78
2	BGR-2	Reinkenhagen	-	-26.8	-26.5	-2.68	0.57	0.49	0.93	0.25	0.25	0.87	0.63	0.84
2	BGR-3	Barth	-	-27.1	-26.2	-1.25	0.55	0.48	0.87	0.35	0.24	0.99	0.94	0.84
2	BGR-4	Grimmen	-	-27.5	-25.1	2.2	0.52	0.57	1.16	0.19	0.25	0.85	0.80	0.76
3	PL-1	Blotno	3181.5-3184	-26.8	-26.1	-1.78	0.42	0.37	0.83	0.14	0.39	0.76	0.45	0.91
3	PL-2	Daszewo	2891.8-2910	-27	-26.6	-2.29	0.17	0.09	0.59	0.21	0.77	0.44	1.17	0.85
3	PL-3	Daszewo N	2842.5-2843.3	-26.2	-25.8	-2.64	0.34	0.18	0.69	0.34	0.46	0.53	1.8	1.06
3	PL-8	Kamień Pomorski	2232	-27.3	-25.9	-0.07	0.54	0.49	1	0.04	0.5	0.7	0.79	0.83
3	PL-9	Kamień Pomorski	2246	-27.4	-26	-0.09	0.45	0.44	0.96	0.06	0.5	0.77	0.81	0.84
3	PL-11	Międzyzdroje	2824.5-2836.5	-27.2	-26.5	-1.66	0.11	0.11	1.27	0.1	0.36	0.72	1.3	0.26
3	PL-15	Rekowo	2666-2667	-26.6	-26.1	-2.29	0.59	0.86	0.99	0.1	0.41	0.58	0.84	0.67
3	PL-22	Wapnica	3015-3029	-27.4	-26.5	-1.16	0.24	0.29	1.24	0.11	0.46	0.76	0.88	0.59
3	PL-23	Wysoka Kamieńska	3030	-27.4	-26.2	-0.37	0.47	0.44	0.96	0.07	0.58	0.69	0.78	0.76
4	BGR-5	Fallstein	-	-27.2	-26.2	-1	0.63	0.42	0.74	0.21	0.23	0.77	0.59	0.86
4	BGR-10	Mittweide	-	-26.7	-26.1	-2.04	0.57	0.45	0.88	0.23	0.26	0.85	0.82	0.85
4	BGR-11	Pillgram	-	-27.2	-26.2	-1	0.57	0.47	0.93	0.23	0.26	0.84	0.92	0.83
4	BGR-15	Schleppzig	-	-27.6	-26.1	0.24	0.60	0.42	0.83	0.23	0.26	0.74	0.90	0.88
5	PL-16	Retno	1700-1730	-27.3	-27.1	-2.74	0.53	0.37	0.64	0.49	0.4	0.56	2.4	0.52
5	PL-20	Struga	2042.5-2058.5	-27.6	-27.6	-3.09	0.38	0.17	0.54	0.51	0.44	0.45	2.79	0.62
6	BGR-9	Kietz	-	-26.5	-25.8	-1.88	0.65	0.41	0.71	0.44	0.27	1.13	0.4	1.1
6	PL-24	Namyślin	3140	-26.4	-25.4	-1.25	0.63	0.44	0.71	0.24	0.67	0.98	0.54	1.19
7	PL-18	Ślawoborze	3242-3258	-27.9	-27.8	-2.86	0.61	0.19	0.47	2.66	0.56	0.78	3.17	0.54
7	PL-19	Ślawoborze	3207-3238	-28.1	-27.9	-2.38	0.43	0.17	0.52	2.94	0.64	0.85	2.35	1.15
8	BGR-6	Volkenroda	-	-28.7	-28.6	-2.53	0.94	0.50	0.63	1.94	0.27	0.87	2.21	1
8	BGR-7	Altengoltern	-	-28.5	-29.2	-4.37	1.21	0.35	0.37	2.25	0.24	0.65	2.11	1.22
8	BGR-8	Mehrstedt	-	-29.2	-28.3	-0.6	0.99	0.56	0.68	1.71	0.26	0.79	2.09	1.07
9	PL-4	Gorzysław	2417-2420.5	-30.6	-30.6	-2.16	0.5	0.78	1.5	0.98	0.33	0.5	1.94	1.19
9	PL-5	Gorzysław	2728-2746	-30.5	-31.0	-3.31	0.7	1.17	1.43	0.82	0.33	0.51	1.96	0.44
9	PL-12	Moracz	3279.5-3309.5	-30.5	-30.1	-1.31	0.27	0.18	0.89	1.33	0.42	0.7	1.89	0.67
9	PL-13	Petrykozy	2623	-30.3	-29.9	-2.26	0.7	0.56	0.91	0.4	0.44	0.79	2.29	0.87
9	PL-21	Wapnica	2812.5-2818.5	-29.9	-29.9	-1.37	0.76	0.57	0.84	1.77	0.46	0.63	1.94	0.72
10	PL-10	Maszewo	1657-1666	-26.3	-26	-2.83	0.15	0.08	0.73	0.39	0.39	0.65	1.92	1.16
10	PL-14	Połęcko	1560.4-1576.9	-26.6	-26	-2.07	0.39	0.33	0.8	0.29	0.3	0.77	1.64	0.71
10	PL-17	Rybaki	1668-1708.5	-25.9	-25.6	-2.95	0.48	0.45	0.8	0.27	0.31	0.81	1.37	0.5

BNH/H	C <sub>29</sub> /H	C <sub>30</sub> dia/H	C <sub>31</sub> R/H	G/C <sub>30</sub>	HHI	C <sub>32</sub> /C <sub>31</sub> (S+R)	C <sub>34</sub> /C <sub>33</sub> (S+R)	C <sub>35</sub> S/C <sub>34</sub> S	%C <sub>31</sub>	%C <sub>32</sub>	%C <sub>33</sub>	%C <sub>34</sub>	%C <sub>35</sub>
0	0.65	0.05	0.38	0.14	0.13	0.84	1.01	0.89	32	27	14	14	13
0	0.67	0.04	0.43	0.15	0.13	0.93	1.21	0.74	29	27	14	17	13
0	0.8	0.05	0.42	0.15	0.13	0.76	0.89	1.02	35	26	14	13	13
0.07	0.48	0.08	0.54	0.24	0.16	0.87	1.38	0.76	26	23	15	20	16
0.07	0.66	0.11	0.64	0.21	0.12	1.02	1.11	0.77	29	30	14	15	12
0	0.39	0.03	0.39	0.19	0.23	0.99	1.17	1.19	21	21	16	19	23
0	0.42	0.03	0.38	0.16	0.19	0.89	1.10	1.04	25	22	16	18	19
0	0.37	0.03	0.38	0.18	0.22	0.98	1.11	1.17	21	21	17	19	22
0	0.39	0.03	0.37	0.16	0.21	0.93	1.16	1.11	23	21	16	19	21
0.03	0.68	0.07	0.46	0.35	0.26	0.82	1.07	1.56	23	18	16	17	26
0.03	0.94	0.04	0.48	0.21	0.25	0.84	1.2	1.47	24	20	14	17	25
0	0.65	0.06	0.48	0.14	0.18	0.95	1.41	0.94	25	24	14	19	18
0.01	0.62	0.02	0.36	0.17	0.21	0.87	0.72	1.38	24	21	16	16	23
0.01	0.63	0.02	0.36	0.18	0.24	0.86	0.72	1.37	24	21	16	16	23
0.01	0.59	0.01	0.41	0.25	0.31	1.02	1.25	1.7	18	18	15	18	31
0.03	0.65	0.03	0.44	0.23	0.29	0.86	1.1	1.71	21	18	15	17	29
0.02	0.56	0.03	0.39	0.24	0.3	1.02	1.2	1.65	18	18	15	18	30
0.01	0.57	0.03	0.37	0.2	0.26	0.88	0.72	1.4	23	20	17	17	23
0	0.56	0.03	0.4	0.13	0.12	0.64	1.10	0.74	34	22	15	17	12
0	0.5	0.03	0.42	0.13	0.15	0.73	0.93	0.96	30	22	17	16	15
0	0.49	0.03	0.41	0.10	0.14	0.75	0.92	0.92	30	23	17	16	14
0	0.57	0.04	0.39	0.12	0.16	0.70	0.99	0.99	31	21	16	16	16
0.06	0.54	0.07	0.5	0.23	0.17	0.87	1.22	0.89	27	23	15	18	17
0.06	0.71	0.07	0.51	0.27	0.17	0.81	1.44	0.75	26	21	15	21	17
0	2.03	0	0	0.00	0	0.00	0.00	0	0	0	0	0	0
0.06	0.84	0.2	0.15	0.20	0	0.55	0	0	54	30	16	0	0
0.21	5.78	0	1.67	0	0	0	0	0	100	0	0	0	0
0.18	4.36	0	1.1	0	0	0	0	0	100	0	0	0	0
0	0.41	0.03	0.37	0.19	0.14	1.01	1.14	0.77	26	26	16	18	14
0	0.68	0.04	0.42	0.20	0.13	0.79	2.04	0.39	26	20	13	27	13
0	0.43	0.03	0.34	0.20	0.13	0.95	1.09	0.70	28	26	16	17	13
0.05	0.57	0.16	0.56	0.41	0.26	1.12	1.27	1.48	21	23	13	17	26
0.04	0.31	0.08	0.56	0.35	0.24	1.04	1.32	1.28	22	23	14	18	24
0.01	0.4	0.28	0.36	0.19	0.27	1.06	1.08	1.59	19	21	16	17	27
0.02	0.4	0.18	0.34	0.11	0.27	1	0.78	1.31	23	23	15	17	22
0.03	0.38	0.29	0.34	0.2	0.25	1.07	1.01	1.43	20	21	17	17	25
0.03	0.51	0.07	0.51	0.23	0.17	0.91	1.14	0.94	27	24	15	17	17
0.02	0.49	0.06	0.58	0.22	0.18	0.81	1.02	1.05	28	22	16	16	18
0.05	0.39	0.06	0.53	0.2	0.16	0.78	1	0.97	29	22	16	16	16



C <sub>29</sub> dia/(dia+reg)	C <sub>27</sub> dia/(dia+reg)	%C <sub>27</sub>	%C <sub>28</sub>	%C <sub>29</sub>	C <sub>27</sub> /C <sub>29</sub>	C <sub>28</sub> /C <sub>29</sub>	tricyclics/17 $\alpha$ -hopanes	steranes/17 $\alpha$ -hopanes	ISO	CHL	DBT/P	CPI
0.22	0.12	25	24	51	0.49	0.46	0.16	0.52	45	12	2.32	0.93
0.31	0.22	31	19	51	0.61	0.37	0.15	0.17	nd	nd	3.52	0.94
0.32	0.23	31	21	48	0.65	0.44	0.30	0.26	49	nd	5.08	0.99
0.15	0.34	37	20	43	0.7	0.47	0.06	0.18	60	4	2.97	0.93
0.32	0.42	47	13	40	0.91	0.48	0.03	0.1	16	1	3.24	0.91
0.32	0.32	30	19	51	0.59	0.36	0.10	0.79	408	65	0.09	0.88
0.24	0.24	27	21	52	0.53	0.39	0.16	0.91	163	27	0.24	0.91
0.28	0.26	27	21	52	0.51	0.41	0.15	1.01	159	27	0.47	0.92
0.24	0.22	25	22	53	0.48	0.42	0.10	0.92	360	47	0.15	0.89
0.14	0.29	37	23	40	0.69	0.51	0.15	0.28	161	9	11.5	0.99
0.11	0.22	41	23	36	0.87	0.54	0.09	0.17	73	4	3.46	0.93
0.27	0.34	50	18	32	0.98	0.51	0.05	0.12	23	nd	1.5	0.92
0.17	0.17	24	26	50	0.48	0.52	0.11	0.34	275	44	2.62	0.96
0.17	0.17	23	26	51	0.45	0.51	0.11	0.32	22	3	2.59	0.98
0.04	0.12	26	24	50	0.47	0.57	0.05	0.35	585	26	3.02	0.94
0.05	0.17	28	26	46	0.52	0.41	0.06	0.29	320	19	4.33	0.93
0.05	0.15	29	22	49	0.51	0.32	0.06	0.35	710	26	2.58	0.94
0.21	0.17	24	27	49	0.49	0.55	0.11	0.32	117	53	0.64	0.97
0.2	0.12	20	25	55	0.36	0.45	0.50	2.04	58	21	1.00	0.97
0.24	0.20	24	24	52	0.46	0.46	0.32	1.15	125	19	0.62	0.91
0.27	0.24	27	22	51	0.52	0.43	0.18	0.71	230	27	0.98	0.91
0.18	0.12	22	25	53	0.41	0.47	0.26	1.37	145	17	1.27	0.96
0.17	0.42	28	23	49	0.53	0.53	0.05	0.17	50	nd	9.24	0.91
0.20	0.41	35	20	45	0.66	0.48	0.05	0.12	46	4	7.13	0.92
0.49	0.42	39	19	42	0.93	0.46	5.32	1.83	nd	nd	1.39	0.98
1.98	0.28	32	32	36	0.89	0.89	0.53	0.65	nd	nd	1.22	0.99
2.99	0.58	75	11	13	4.45	1.36	0.53	1.07	nd	nd	14.47	0.95
3.02	0.65	75	10	15	3.55	1.42	0.49	0.75	nd	nd	13.18	0.94
0.54	0.34	43	14	43	0.98	0.33	0.27	0.52	nd	nd	1.18	0.95
0.62	0.32	47	14	38	1.23	0.37	1.47	1.04	nd	nd	0.24	0.98
0.54	0.35	43	14	43	1.01	0.32	0.23	0.43	nd	nd	0.65	0.96
0.29	0.48	39	13	49	0.44	0.38	0.04	0.31	nd	nd	2.78	0.85
0.33	0.5	41	11	48	0.58	0.4	0.04	0.27	nd	nd	1.81	0.88
0.78	0.48	68	9	23	1.68	0.86	0.14	0.37	nd	nd	6.85	0.95
0.47	0.33	44	10	46	0.33	0.31	0.1	0.2	nd	nd	0.25	0.92
0.76	0.44	70	7	23	1.72	0.83	0.15	0.36	nd	nd	2.32	0.94
0.18	0.36	36	21	43	0.64	0.48	0.06	0.23	141	6	7.56	0.93
0.15	0.38	34	22	44	0.62	0.52	0.06	0.28	234	6	3.63	0.93
0.16	0.37	35	21	44	0.64	0.48	0.07	0.32	341	14	4.27	0.93

Table 1. Source-related geochemical characteristics of Ca2 oil samples.

nd – not determined;

$\delta^{13}\text{C}_{\text{SAT}}$  – stable carbon isotopic composition (‰) of the saturated hydrocarbon fraction;

$\delta^{13}\text{C}_{\text{ARO}}$  – stable carbon isotopic composition (‰) of the aromatic hydrocarbon fraction;

CV – canonical variable ( $\text{CV} = -2.53\delta^{13}\text{C}_{\text{SAT}} + 2.22\delta^{13}\text{C}_{\text{ARO}} - 11.65$ );

- 1060 Pr/Ph – pristane/phytane;
- 1061 Pr/*n*-C<sub>17</sub> – pristane/*n*-heptadecane;
- 1062 Ph/*n*-C<sub>18</sub> – phytane/*n*-octadecane;
- 1063 C<sub>19</sub>/C<sub>23</sub> – C<sub>19</sub>/C<sub>23</sub> tricyclic terpanes;
- 1064 C<sub>22</sub>/C<sub>21</sub> – C<sub>22</sub>/C<sub>21</sub> tricyclic terpanes;
- 1065 C<sub>24</sub>/C<sub>23</sub> – C<sub>24</sub>/C<sub>23</sub> tricyclic terpanes;
- 1066 C<sub>24</sub>Tet/C<sub>23</sub> – C<sub>24</sub> tetracyclic/C<sub>23</sub> tricyclic terpanes;
- 1067 C<sub>26</sub>/C<sub>25</sub> – C<sub>26</sub>/C<sub>25</sub> tricyclic terpanes;
- 1068 BNH/H – 28,30-bisnorhopane / C<sub>30</sub> 17 $\alpha$ -hopane;
- 1069 C<sub>29</sub>/H – C<sub>29</sub> norhopane / C<sub>30</sub> 17 $\alpha$ -hopane;
- 1070 C<sub>30</sub> dia/H – C<sub>30</sub> diahopane / C<sub>30</sub> 17 $\alpha$ -hopane;
- 1071 C<sub>31</sub>R/H – C<sub>31</sub> homohopane 22R / C<sub>30</sub> 17 $\alpha$ -hopane;
- 1072 G/H – gammacerane / C<sub>30</sub> 17 $\alpha$ -hopane;
- 1073 HHI – homohopane index: C<sub>35</sub> $\alpha\beta$ (S + R) / ( $\Sigma$ C<sub>31</sub>-C<sub>35</sub> $\alpha\beta$  S + R);
- 1074 C<sub>32</sub>/C<sub>31</sub> (S+R) – C<sub>32</sub> (S+R) 17 $\alpha$ -hopane / C<sub>31</sub> (S+R) 17 $\alpha$ -hopane;
- 1075 C<sub>34</sub>/C<sub>33</sub> (S+R) – C<sub>34</sub> (S+R) 17 $\alpha$ -hopane / C<sub>33</sub> (S+R) 17 $\alpha$ -hopane;
- 1076 C<sub>35</sub>S/C<sub>34</sub>S – C<sub>35</sub>S/C<sub>34</sub>S homohopanes;
- 1077 %C<sub>31</sub>, %C<sub>32</sub>, %C<sub>33</sub>, %C<sub>34</sub>, %C<sub>35</sub> – percentage of C<sub>31</sub>, C<sub>32</sub>, C<sub>33</sub>, C<sub>34</sub>, C<sub>35</sub> to total C<sub>31-35</sub> homohopanes;
- 1078 C<sub>29</sub> dia – diasterane/sterane ratio – C<sub>29</sub> 13 $\beta$ ,17 $\alpha$ (H) (20S + 20R) / (C<sub>29</sub> 5 $\alpha$ ,14 $\alpha$ ,17 $\alpha$ (H) 20S + 20R + 5 $\alpha$ ,14 $\beta$ ,17 $\beta$ (H) 20S + 20R);
- 1080 %C<sub>27</sub> (*m/z* 217) – 100 x C<sub>27</sub>S / (C<sub>27</sub>S + C<sub>28</sub>S + C<sub>29</sub>S);
- 1081 %C<sub>28</sub> (*m/z* 217) – 100 x C<sub>28</sub>S / (C<sub>27</sub>S + C<sub>28</sub>S + C<sub>29</sub>S);
- 1082 %C<sub>29</sub> (*m/z* 217) – 100 x C<sub>29</sub>S / (C<sub>27</sub>S + C<sub>28</sub>S + C<sub>29</sub>S);
- 1083 C<sub>27</sub>/C<sub>29</sub> – C<sub>27</sub>/C<sub>29</sub> sterane ratio;
- 1084 C<sub>28</sub>/C<sub>29</sub> – C<sub>28</sub>/C<sub>29</sub> sterane ratio;
- 1085 tricyclics/17 $\alpha$ -hopanes –  $\Sigma$ C<sub>19-26</sub> tricyclic terpanes / ( $\Sigma$ C<sub>19-26</sub> tricyclic terpanes +  $\Sigma$ C<sub>29-33</sub> 17 $\alpha$ -hopanes);
- 1086 steranes/17 $\alpha$ -hopanes –  $\Sigma$ C<sub>27-29</sub> regular steranes /  $\Sigma$ C<sub>28-35</sub> 17 $\alpha$ -hopanes;
- 1087 ISO – isorenieratane ( $\mu$ g/g oil);
- 1088 CHL – chlorobactane ( $\mu$ g/g oil);
- 1089 DBT/P – dibenzothiophene/phenanthrene;
- 1090 CPI – carbon preference index based on *n*-alkanes [ $\Sigma$ (C<sub>25</sub>–C<sub>33</sub>)<sub>odd</sub> /  $\Sigma$ (C<sub>24</sub>–C<sub>32</sub>)<sub>even</sub> +  $\Sigma$ (C<sub>25</sub>–C<sub>33</sub>)<sub>odd</sub> /  $\Sigma$ (C<sub>26</sub>–C<sub>34</sub>)<sub>even</sub>] / 2
- 1092
- 1093

Group	Wells	C <sub>27</sub> Ts/Tm	M/H	C <sub>29</sub> 20S	C <sub>29</sub> $\beta\beta$	TA(I)/TA(I+II)	MDR	Rm
1	BGR-12	1.14	0.12	0.51	0.57	0.23	2.98	0.73
1	BGR-13	1.36	0.14	0.45	0.55	0.25	2.52	0.69
1	BGR-14	2.44	0.18	0.49	0.55	0.55	3.32	0.75
1	PL-6	1.43	0.1	0.47	0.58	0.26	2.10	0.72
1	PL-7	1.11	0.13	0.43	0.56	0.16	1.96	0.71

2	BGR-1	0.87	0.10	0.50	0.54	0.05	5.89	0.94
2	BGR-2	0.95	0.09	0.48	0.53	0.06	3.24	0.75
2	BGR-3	1.3	0.07	0.49	0.58	0.12	2.51	0.69
2	BGR-4	0.73	0.10	0.50	0.54	0.04	4.04	0.80
3	PL-1	3.5	0.06	0.51	0.57	0.30	2.18	0.72
3	PL-2	1.1	0.09	0.5	0.59	0.22	2.65	0.74
3	PL-8	0.92	0.05	0.54	0.53	0.14	1.58	0.63
3	PL-9	0.91	0.06	0.56	0.52	0.12	2.04	0.66
3	PL-11	0.63	0.06	0.47	0.56	0.1	1.76	0.70
3	PL-15	0.98	0.07	0.48	0.56	0.08	1.78	0.70
3	PL-22	0.77	0.08	0.48	0.57	0.11	1.76	0.70
3	PL-23	1.23	0.1	0.55	0.57	0.09	3.30	0.75
4	BGR-5	1.13	0.09	0.49	0.58	0.11	3.90	0.79
4	BGR-10	1.26	0.12	0.51	0.58	0.24	3.63	0.78
4	BGR-11	0.9	0.10	0.50	0.58	0.32	2.51	0.69
4	BGR-15	0.79	0.10	0.51	0.59	0.16	3.55	0.77
5	PL-3	0.77	0.11	0.53	0.58	0.2	2.16	0.72
5	PL-16	1.85	0.1	0.46	0.58	0.21	1.76	0.70
5	PL-20	1.42	0.1	0.47	0.56	0.24	2.05	0.71
6	BGR-9	5.23	nd	0.50	0.59	0.83	3.76	0.78
6	PL-24	2.13	nd	nd	nd	nd	2.98	0.73
7	PL-18	11.77	nd	nd	0.55	1.00	4.91	0.91
7	PL-19	10.9	nd	nd	0.57	1.00	4.53	0.85
8	BGR-6	0.81	0.08	0.51	0.59	0.41	5.54	0.91
8	BGR-7	0.94	0.17	0.50	0.57	1	8.31	1.12
8	BGR-8	1.32	0.09	0.50	0.59	0.39	5.64	0.92
9	PL-4	0.76	0.19	0.49	0.57	0.10	1.59	0.68
9	PL-5	0.83	0.09	0.48	0.55	0.08	1.48	0.67
9	PL-12	4.01	0.15	0.5	0.61	0.38	2.59	0.74
9	PL-13	1.95	0.08	0.56	0.52	0.19	1.80	0.64
9	PL-21	2.99	0.16	0.51	0.62	0.36	3.77	0.78
10	PL-10	1.55	0.12	0.48	0.56	0.19	1.72	0.69
10	PL-14	1.17	0.11	0.47	0.55	0.12	1.63	0.69
10	PL-17	1.4	0.1	0.44	0.54	0.13	1.82	0.70

Table 2. Selected biomarker maturity and maturity-controlled parameters for Ca2 oil samples.

nd – not determined;

$C_{27}$  Ts/Tm –  $C_{27}$  18 $\alpha$ -trisnorhopane / 17 $\alpha$ -trisnorhopane;

M/H – moretane/hopane;

$C_{29}$  20S – 20S / (20S + 20R) epimers of 5 $\alpha$ (H),14 $\alpha$ (H),17 $\alpha$  $\beta$ (H)-ethylsterane;

$C_{29}$   $\beta\beta$  – 5 $\alpha$ (H),14 $\beta$ (H),17 $\beta$ (H)/[5 $\alpha$ (H),14 $\beta$ (H),17 $\beta$ (H) + 5 $\alpha$ (H),14 $\alpha$ (H),17 $\alpha$ (H) 20R ethylsteranes];

1102  $TA(I)/TA(I+II) - TA(I) = C_{20}+C_{21}$ ,  $TA(II) = \Sigma C_{26}-C_{28}$  (20S + 20R) triaromatic steroids;

1103 MDR – methyl dibenzothiophene ratio = 4-MDBT / 1-MDBT;

1104  $R_m$  – calculated vitrinite reflectance =  $0.073 \times MDR + 0.51$

1105

1106